Consequences of thrusting and intraplate stress fluctuations for vertical motions in foreland basins and peripheral areas

Peper, T.; Beekman, F.; Cloetingh, S.A.P.L.

published in
Geophysical Journal International
1992

DOI (link to publisher)
10.1111/j.1365-246X.1992.tb00558.x

document version
Publisher's PDF, also known as Version of record

Geophys. J. Int. (1992) **111**, 104–126

Consequences of thrusting and intraplate stress fluctuations for vertical motions in foreland basins and peripheral areas

Tim Peper, Fred Beekman and Sierd Cloetingh
Institute of Earth Sciences, Vrije Universiteit, De Boelelaan 1085, 1081 HV Amsterdam, The Netherlands

Accepted 1992 April 8. Received 1992 April 8; in original form 1991 May 31

SUMMARY

We present a conceptual model for short-term and long-term alternations in subsidence and uplift in foreland basins. Convergence of lithospheric plates produces forces at the plate boundaries, generating stresses in the accretionary wedge, the underthrusted crust, and the lithosphere. When the stresses reach the shear strength of the rocks in these units, deformation, which results in the redistribution of mass, takes place contemporaneously with reduction of the stress level. Modelling of both the effects of this alternating building up and relaxation of stress, and the effects of the resulting mass redistribution on foreland basin geometry, employing an elastic rheology of the lithosphere, demonstrates that these processes exert an important control on the shape of foreland basins. Vertical motions take place on different time-scales dependent on the scale of thrusting and the style of deformation. Short-term (10–10^4 yr) vertical motions are related to small-scale thrust events, while long-term vertical motions are induced by larger scale deformation in the overriding thrust wedge. Furthermore, the geometry of faults influences the duration of the magnitude of stress fluctuations.

Stress-induced alternations of subsidence may lead to the deposition of alternating sequences in foreland basins on scales of centimetres (e.g. cyclothems) to scales of several hundreds of metres (on-lap and off-lap sequences). In this respect, the mechanical coupling between convergent zones and peripheral areas is of particular importance, as it induces simultaneous alternations in regional facies patterns. The model also provides an explanation for vertical motions in the foreland basin previously attributed to visco-elastic relaxation processes.

Key words: facies changes, foreland, stress fluctuations, thrusting.

INTRODUCTION

During the last decade there has been much discussion on the geological processes that lead to the formation of vertically alternating sequences in sedimentary basins. The alternating strata represent facies transitions that are the consequence of allocyclic sedimentary processes (e.g. Galloway 1989) or relative sea-level changes. One of the major points of debate is whether the relative sea-level fluctuations are due to eustasy (e.g. Vail, Mitchum & Thompson 1977; Van Wagoner *et al.* 1990) or due to tectonic events (e.g. Cloetingh 1988, 1991; Angevine 1989; Flemmings & Jordan 1989). Another topic of discussion is which rheological model should be used in the interpretation of the tectonically related sequences. Of the possible models for the rheological properties of the lithosphere, the elastic model and the visco-elastic model are the most frequently used in sedimentary basin analyses (e.g. Watts, Karner & Steckler 1982). None of these models, however, has yet satisfactorily explained the spectrum of stratigraphic observations in foreland basins.

Foreland basin sedimentation patterns record many facies transitions on different time-scales, which have been related to both eustatic sea-level fluctuations and tectonic processes. Short-term sequences, that span tens to thousands of years, have been related to Milankovitch and other types of eustatic sea-level cycles (e.g. Berger *et al.* 1984; Anderson, Goodwin & Sobieski 1984) in the absence of a tectonic model that explains high frequent vertical motions of the lithosphere. Longer term sequences have been interpreted in terms of eustatic sea-level rises and falls (Vail *et al.* 1977; Posamentier, Jervey & Vail 1988; Van Wagoner *et al.* 1990), thrust nappe displacement (Jordan 1981; Cant & Stockmal 1989) and visco-elastic behaviour of the lithosphere (Beaumont 1981; Quinlan & Beaumont 1984). The discussion on the visco-elastic behaviour of the lithosphere

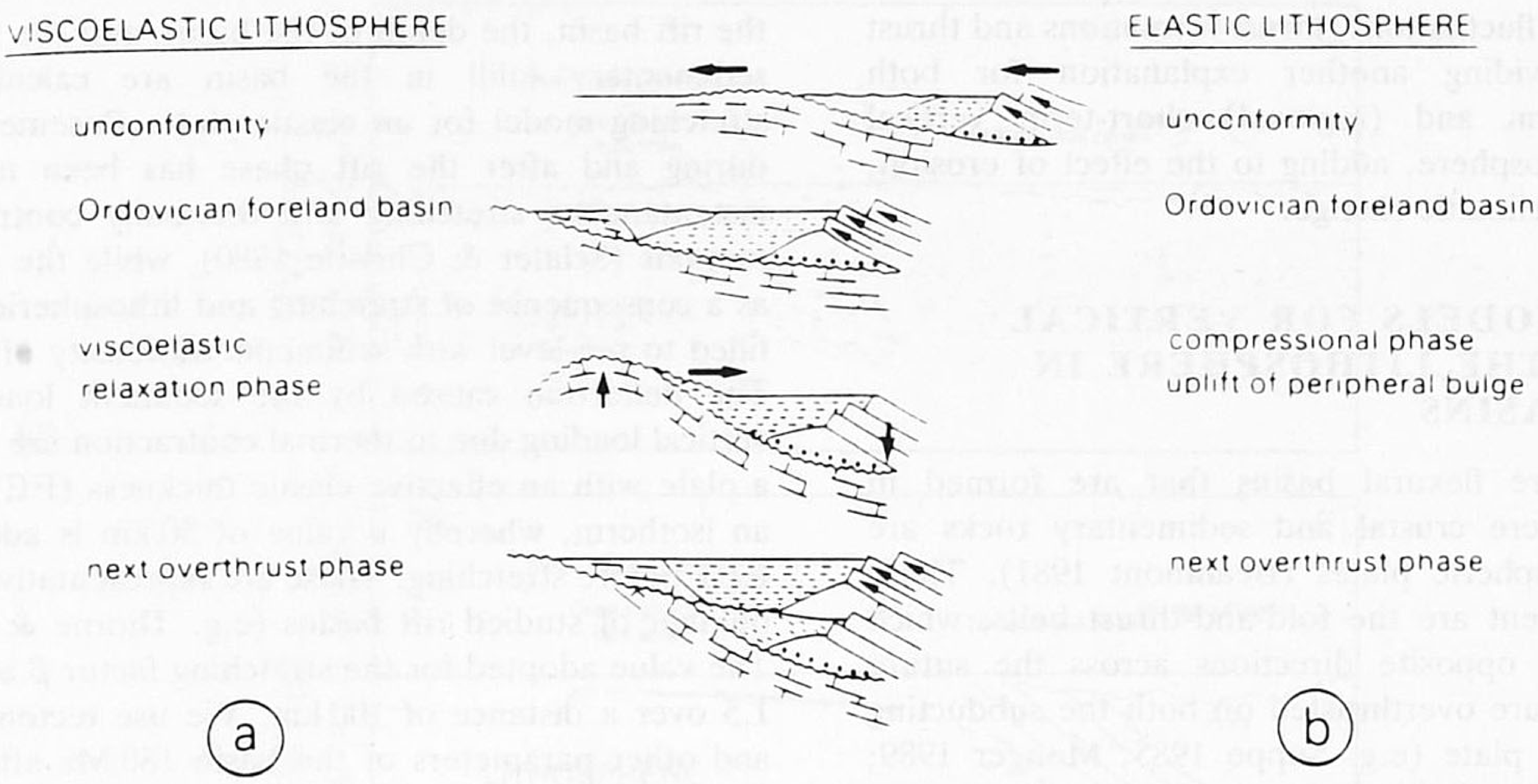

Figure 1. Model for the multistage Appalachian foreland basin. The left column (a) shows a visco-elastic model for the motions in the basin (after Quinlan & Beaumont 1984). The right column (b) shows a model with tectonic intraplate stress fluctuations (after Cloetingh 1988). Bold arrows show overthrust and peripheral bulge migration, fine arrows mark active overthrusting. Both models can explain the basinward migration of the peripheral bulge during a period of apparent tectonic quiescence. The visco-elastic model predicts basinward migration with visco-elastic relaxation of bending stresses which accumulated during an earlier phase of thrusting. The model with tectonic intraplate stress fluctuations predicts basinward migration of the bulge in times of increasing intraplate stress affecting the flexural equilibrium of the lithosphere. Stresses accumulate when thrust displacement is slowed down and a period of apparent tectonic quiescence starts. Stress relaxation occurs upon thrusting.

amongst others focuses on observations of occasionally drowning of the foothills—the area at the front of the pile of thrust nappes—contemporaneously with the rise of the flexural bulge in the Appalachian foreland basin (e.g. Tankard, 1986a,b), and similar features in the Alpine Molasse basin, where the Burdigalian unconformity (e.g. Berger 1985) is related to apparent higher tectonic subsidence rates near the foothills compared to subsidence rates near the flexural bulge (see also Lemcke 1981; Monnier 1979; Mugnier & Menard 1986).

The asymmetry in these facies changes eliminates eustasy as a possible cause for their generation. Modelling studies from Beaumont (1981) and Quinlan & Beaumont (1984) indicated that the stratigraphic patterns in the Appalachians could also not be explained with elastic models. Those models require tectonic activity during deposition of the units, which is in contrast with the observed record. Visco-elastic models as proposed by Courtney & Beaumont (1983), however, could successfully predict both the subsidence of the area around the vertical load and the contemporaneous rise of the flexural bulge, by visco-elastic relaxation of bending stresses in times of tectonic quiescence (see Fig. 1). Therefore, the motions were primarily attributed to visco-elastic behaviour of the lithosphere.

Recent work, however, has shown that some of the observations of foreland basin vertical motions could equally well be explained with elastic models, by incorporating the effects of the interplay between thrusting, erosion, and sediment loading (Flemmings & Jordan 1989), and by incorporating the effects of climatic change (e.g. Beaumont *et al.* 1990). The prime processes herein are erosion and sedimentation, which induce the redistribution of mass, and so a disruption of the flexural equilibrium with time. Other models, with hinterland loading (Sinclair *et al.* 1991) or with lateral changes in the lithospheric strength influencing the flexural response to shortening processes (Stockmal & Beaumont 1987), also provided suitable explanations for the observations of the previously discussed vertical motions.

In all these models the effects of thrusting have been analysed with prolonged progradation of a single triangular-shaped wedge across an underthrusted basement. The overriding wedge, however, is composed of a number of smaller wedges—the thrust nappes. The nappes are discrete units with relatively sharp boundaries, and do not move simultaneously (e.g. Dorobek *et al.* 1992; Searle 1985; Schedl & Dorr 1983; Price, Monger & Muller 1981). This means that with time the location of new thrust loading changes. Using kinematic models with localized thrust loading, we show that, besides erosion and sedimentation, thrusting can also lead to a wide spectrum of vertical motions of the lithosphere with an elastic rheology.

Subsequently, we present the results of modelling the effects of intraplate stress fluctuations. Studies of lithospheric folding and intraplate seismicity (Stein, Cloetingh & Wortel 1990; Stephenson & Cloetingh 1991; Govers *et al.* 1992) have demonstrated the significance of intraplate stresses that can be in the order of several hundreds of MPa, for the deformation of the lithosphere. Furthermore, Cloetingh (1988, 1991) pointed out that temporal changes in the compressional stresses of a much lower magnitude could affect foreland basin geometries. The build up of intraplate stress, for example, could induce a rise of the flexural bulge in times of apparent tectonic quiescence, while subsequent thrusting, attended with a stress relaxation (see also De Bremaecker 1987) could give rise to a cratonward motion of the bulge (Fig. 1). Using numerical models, we investigate the relation between the amplitude and the frequency of the intraplate stress fluctuations and deformation of the lithosphere involved in foreland basin development. The results are integrated in a conceptual model that combines the effects of stress fluctuations, thrust formations and thrust displacement, providing another explanation for both (regional) long-term and (regional) short-term vertical motions of the lithosphere, adding to the effect of erosion, sedimentation and climatic change.

KINEMATIC MODELS FOR VERTICAL MOTIONS OF THE LITHOSPHERE IN FORELAND BASINS

Foreland basins are flexural basins that are formed in collision zones where crustal and sedimentary rocks are displaced on lithospheric plates (Beaumont 1981). These zones of displacement are the fold-and-thrust belts, which generally verge in opposite directions across the suture zone, as the rocks are overthrusted on both the subducting and the overriding plate (e.g. Suppe 1985; Monger 1989; Stern & Davey 1990; ECORS Pyrenees Team 1988, Fig. 2a,b). In this study we focus on the development of foreland basins, that are located on the overriding plate. Because vertical motions of the edge of the overriding plate are restricted by the presence of the subducting plate, we assume that the contact of the overriding and the subducting lithosphere acts as a zone of mechanical coupling (Fig. 2a,b). Therefore, models have been developed with an infinite (elastic) plate (Fig. 3) starting from equations (1) and (2) (see also Bodine 1981).

$$D\frac{\delta^4 w}{\delta x^4} + N\frac{\delta^2 w}{\delta x^2} + (\rho_{\text{mantle}} - \rho_{\text{infill}})gw = q(x), \quad (1)$$

$$D = \frac{ET^3}{12(1-\nu^2)}, \quad (2)$$

where w is the displacement of the lithosphere, D is the flexural rigidity, N is the axial load, ρ is the density, g is the gravity acceleration, q is the vertical load, E is Young's modulus, T is the plate thickness, and ν is Poisson's ratio. Some foreland basins are not lying on (semi) infinite plates, but the principles of changes in stress fields and changes in thrust loads affecting the flexural state of the lithosphere still count. The effect of loading of a broken plate differs from the effect of loading of an infinite plate where the wavelength and the amplitude of the deflection are concerned but, where the bulge migration due to loading is concerned, the changes are basically the same (e.g. Walcott 1976). Furthermore, intraplate stresses affect the flexural state of a broken plate in a rather similar way as for an infinite plate (Appendix).

Many foreland basins are formed close to, or on other basins like former rift zones, where conditions can affect the flexural state of the foreland basin by interference with the flexure of the adjacent basin. Since there are numerous examples of this, like the Appalachian foreland basin, which was located next to the Michigan basin/Mid Continental rift (e.g. Craig & Varnes 1979; De Witt & McCrew 1979), the French western Alps Molasse basin, of which the deposits interfinger with those of the Bresse Graben (Bergerat *et al.* 1989) and others, including the Pyrenees (e.g. ECORS Pyrenees Team 1987) and the Andes (Almendinger *et al.* 1990) foreland basins, we incorporate a peripheral basin in the model. In this study we adopt a symmetrical failed rift basin. The flexural strength of the lithosphere underlying the rift basin, the depth of the basin, and the volume of the sedimentary infill in the basin are calculated with a stretching model for an elastic plate. Basement subsidence during and after the rift phase has been modelled with instantaneous stretching and thermally controlled vertical motions (Sclater & Christie 1980), while the space created as a consequence of stretching and lithospheric cooling, was filled to sea-level with sediments of density of 2400 kg m^{-3}. The deflection caused by the sediment loading and the vertical loading due to thermal contraction are calculated for a plate with an effective elastic thickness (EET) defined by an isotherm, whereby a value of 30 km is adopted for the EET before stretching. These are representative values for a number of studied rift basins (e.g. Thorne & Watts 1989). The value adopted for the stretching factor β amounted 1 to 1.5 over a distance of 100 km. We use tectonic subsidence and other parameters of the basin 180 Ma after stretching. This assumption implies that we eliminate the effect of thermal subsidence of the rift basin in the foreland basin phase. Variations of the EET, other than below the failed rift, are ignored in the absence of accurate EET estimates, including, for example, the effects of thrust nappes on the strength of the overriding plate in collision zones. The effects of erosion and subsequent sedimentation in the basin have been ignored in the present study. Incorporation of the process complicates the effects of lateral redistribution of loads by thrusting and the effects of stress fluctuations, both which are the main focus of this study. We show that the process of thrusting and stress fluctuations can also modify to vertical motions in the foreland basin, giving rise to significant changes in the depositional environment. In the analysis the presence of the peripheral basin is of particular importance.

Models for the effects of thrusting

Vertical motions in foreland basins are dominated by the effect of lateral displacement of thrust nappes (e.g. Jordan 1981; Schedl & Wiltschko 1984). The nappes represent masses that act as loads on the underthrusted lithosphere, which cause deflection and, therefore, control the geometry of the basin formed in front of them. Obviously, the displacement of the thrust nappes—thrust loads—induces changes of the geometry of the foreland basin. We have investigated the effect of the displacement of independent thrust nappes on the flexural state of the lithosphere at discrete time steps, using numerical models that incorporate separate triangular wedges (Fig. 4), that represent displaced crustal loads. Values of 25 and 4 km have been adopted for the height and the width of the wedges, respectively. Emplacement of one wedge is equivalent to 12.5 km progradation of a thrust nappe.

We investigate the effect of the following three types of thrusting: piggy-back thrusting, out-of-sequence thrusting and back thrusting. Of these three thrusting mechanisms, piggy-back thrusting is the best known type (e.g. Boyer & Elliot 1982). This process is characterized by the displacement of nappes across faults that are subsequently formed in the footwall of the former thrust (see also Fig. 4c), and is recognized in, for example, the Sevier fold-and-thrust belt (Armstrong & Oriel 1986). We model a case of piggy-back thrusting, whereby new faults are formed

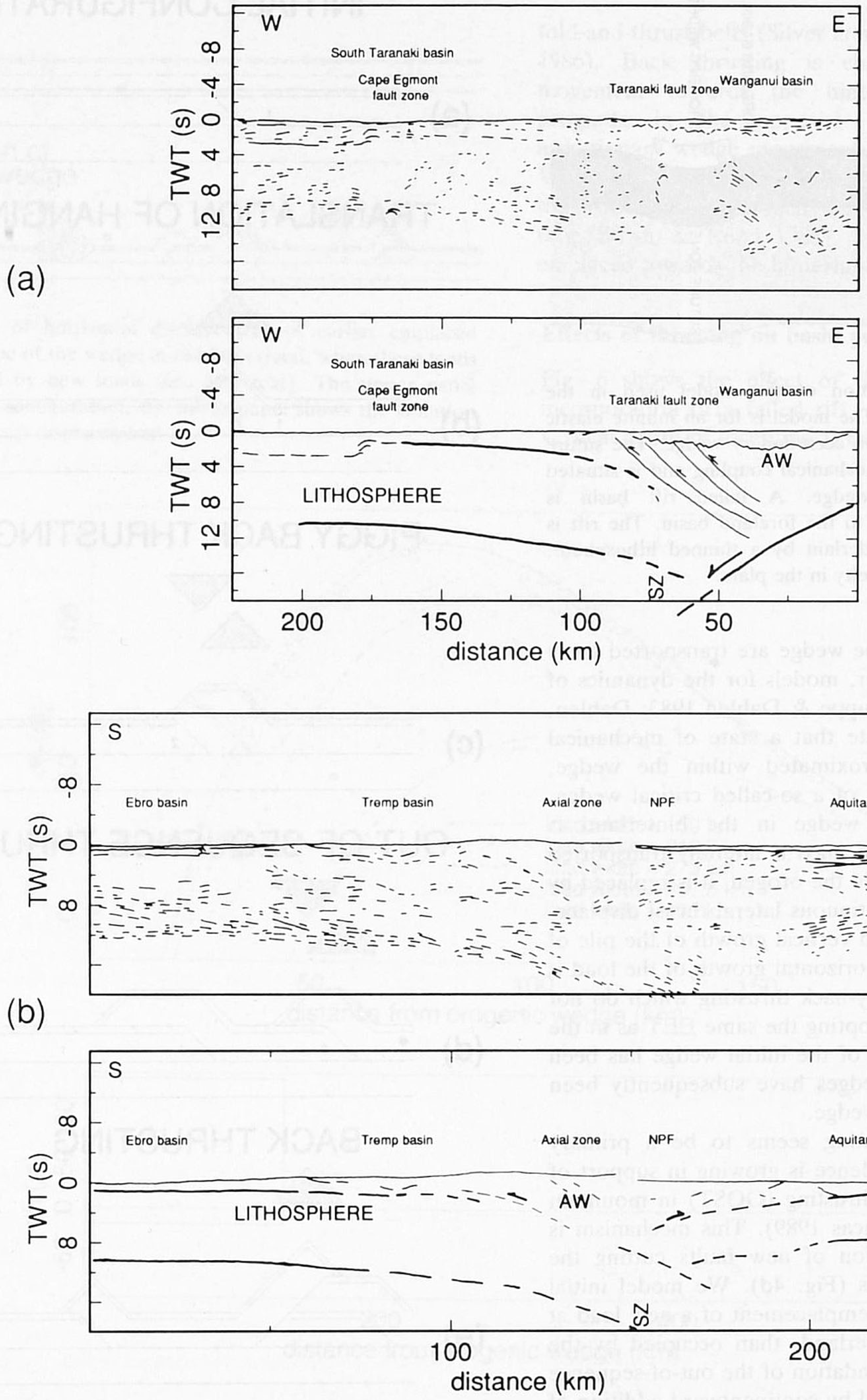

Figure 2. Symmetrical verging fold-and-thrust belt at the Taranaki basin (a), and the Aquitane basin (b). Top figures display seismic data. Bottom figures show interpretation modified after (a) Stern & Davey (1990), and (b) ECORS Pyrenees Team (1988). The foreland basins are formed on the overriding lithosphere. Vertical motions of the lithospheric plates are constrained by the presence of a subducting plate. Annotation: SZ = suture zone; AW = accretionary wedge; NPF = North Pyrenean Fault.

at such locations that motions across the fault are equivalent to emplacement of a wedge next to the earlier emplaced wedges. The model adopts the presence of an initial wedge of 200 km width. The maximum extent of the area in which the effects of successive addition of nappes is modelled, is taken as 350 km, which approaches the width of relatively narrow orogenic zones like the Alpes and the Andes. The displacement across the faults is taken as 12.5 km in this model, while the adopted thrust spacing equals 25 km. These values are representative values for thrust spacing and thrust displacement in piggy-back sequences (e.g. Armstrong & Oriel 1986; Boyer & Elliot 1982).

We neglect the effect of horizontal displacement across the flat basal fault on the distribution of earlier emplaced loads (Fig. 5). Horizontal displacement of earlier emplaced loads causes translation of these loads towards the foreland,

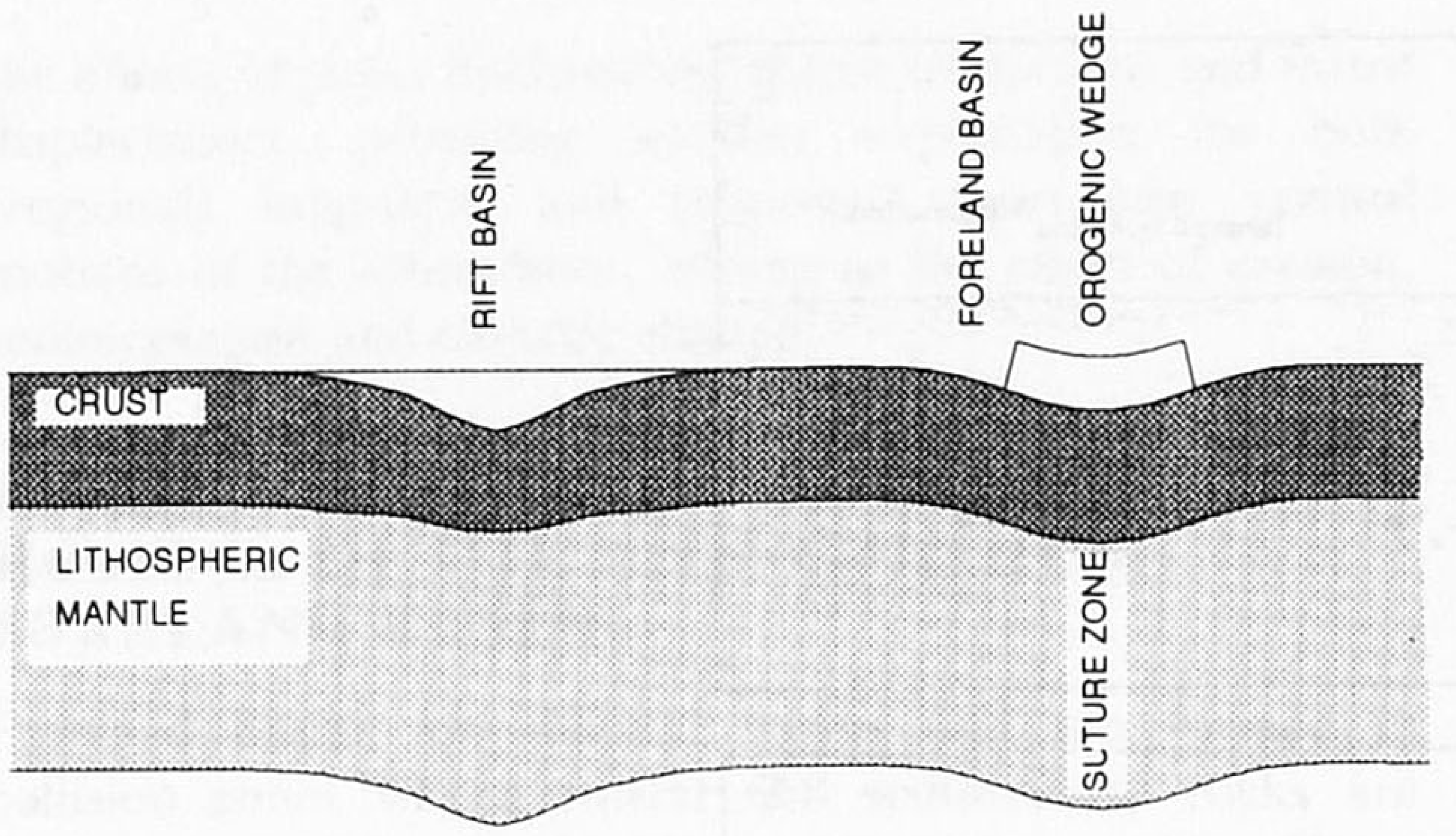

Figure 3. Schematic representation of the model used in the calculations of basin geometry. The model is for an infinite elastic lithosphere that is loaded with an accretionary wedge. The suture zone is regarded as a zone of mechanical coupling and is situated underneath the accretionary wedge. A failed rift basin is incorporated at a location close to the foreland basin. The rift is filled with sediments and is underlain by a thinned lithosphere, forming a mechanical inhomogeneity in the plate.

which implies that parts of the wedge are transported away from the hinterland. However, models for the dynamics of an orogenic wedge (Davis, Suppe & Dahlen 1983; Dahlen, Suppe & Davis 1984) indicate that a state of mechanical dynamic equilibrium is approximated within the wedge, which leads to the formation of a so-called critical wedge. The overall shape of this wedge in the hinterland is constant, and therefore, when mass is laterally transported away from a certain location in the orogen, it is replaced by new mass. Consequently, continuous lateral thrust displacement leads to both lateral and vertical growth of the pile of thrust nappes. The effect of horizontal growth of the load is calculated for models of piggy-back thrusting which do not incorporate the failed rift, adopting the same EET as in the failed rift models. The width of the initial wedge has been taken as 25 km, and new wedges have subsequently been emplaced next to this initial wedge.

Although piggy-back thrusting seems to be a primary mechanism for thrusting, evidence is growing in support of the role of out-of-sequence thrusting (OOST) in mountain belts (Morley 1986, 1988; Lucas 1989). This mechanism is characterized by the formation of new faults cutting the hanging wall of former faults (Fig. 4d). We model initial out-of-sequence thrusting by emplacement of a new load at a location closer to the hinterland, than occupied by the earlier emplaced loads. Progradation of the out-of-sequence thrusted nappes was simulated by continentward addition of loads, adjacent to the initially emplaced new load. The locations of thrust emplacement and thrust formation have been taken at random and the spacing between the faults in the modelling maximally reach values of 50 km. The adopted displacement values are inferred from geological observations, with cases of thrust displacement of several tens of kilometres (Morley 1988; Glacon & Rouvier 1972). The values for the distances between newly formed faults have not extensively been investigated and are, therefore, not well constrained. However, if displacements reach values of 50 or more kilometres, the initial thrust spacing must also have been of this magnitude.

Back thrusting also appears to be of great significance in

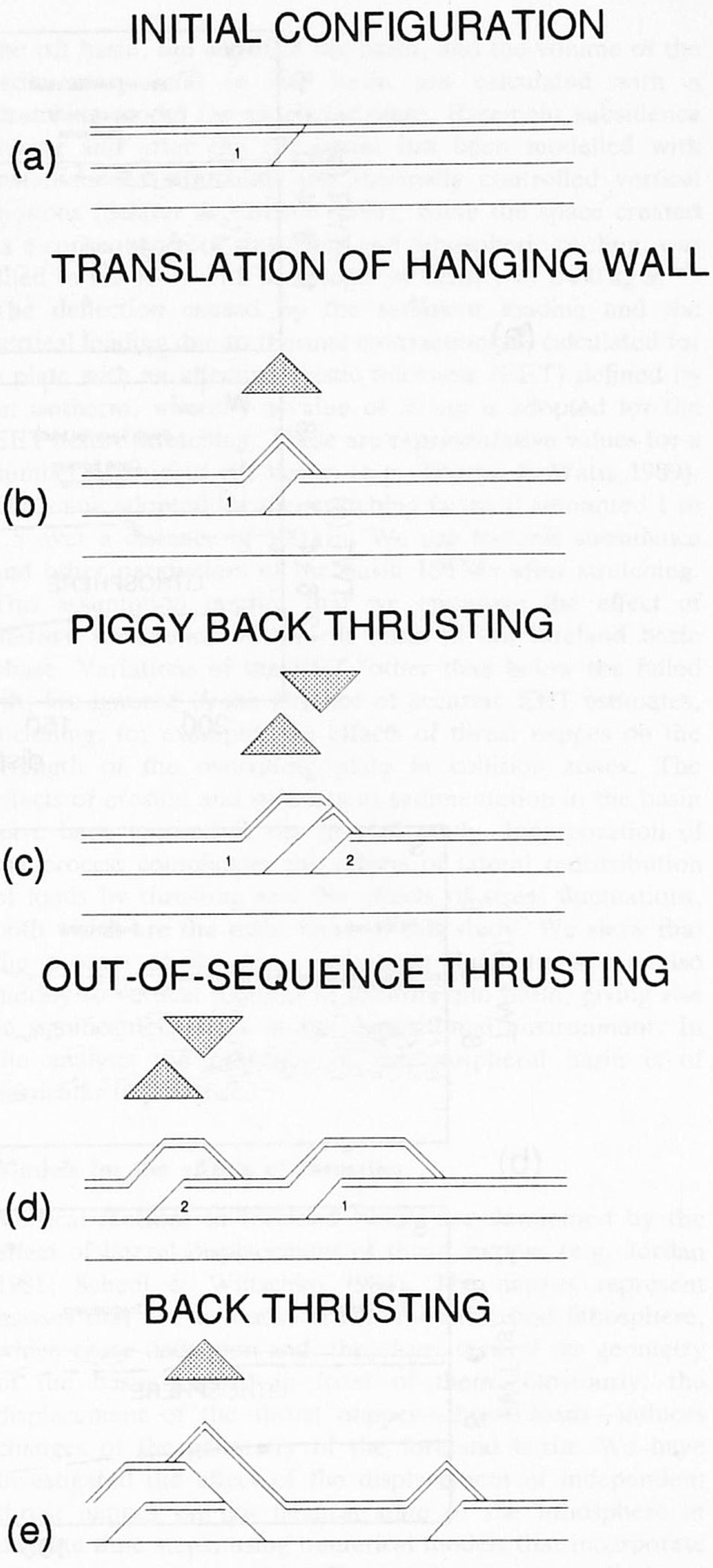

Figure 4. Schematic representation of geometrical effects of thrusting. Faults are limited to the upper layer and involve both thick- and thin-skinned tectonics. Labels mark the order of formation of fault zones in the underthrusted lithosphere. (a) Initial situation before thrusting. (b) Geometrical changes after translation of the hanging wall across fault nr. (1). Thrusting corresponds to emplacement of a triangular wedge on the initial configuration of Fig. 3. (c) Piggy-back thrusting. Adopted thrust zones and translations are at locations and of magnitudes, such that piggy-back thrusting can be regarded as emplacement of triangular wedges adjacent to earlier emplaced wedges. (d) Out-of-sequence thrusting. Thrust nappes are emplaced in the hinterland. (e) Back thrusting. Faults dip to the continent. Back thrusting is regarded as emplacement of new triangular wedges on top of earlier emplaced loads.

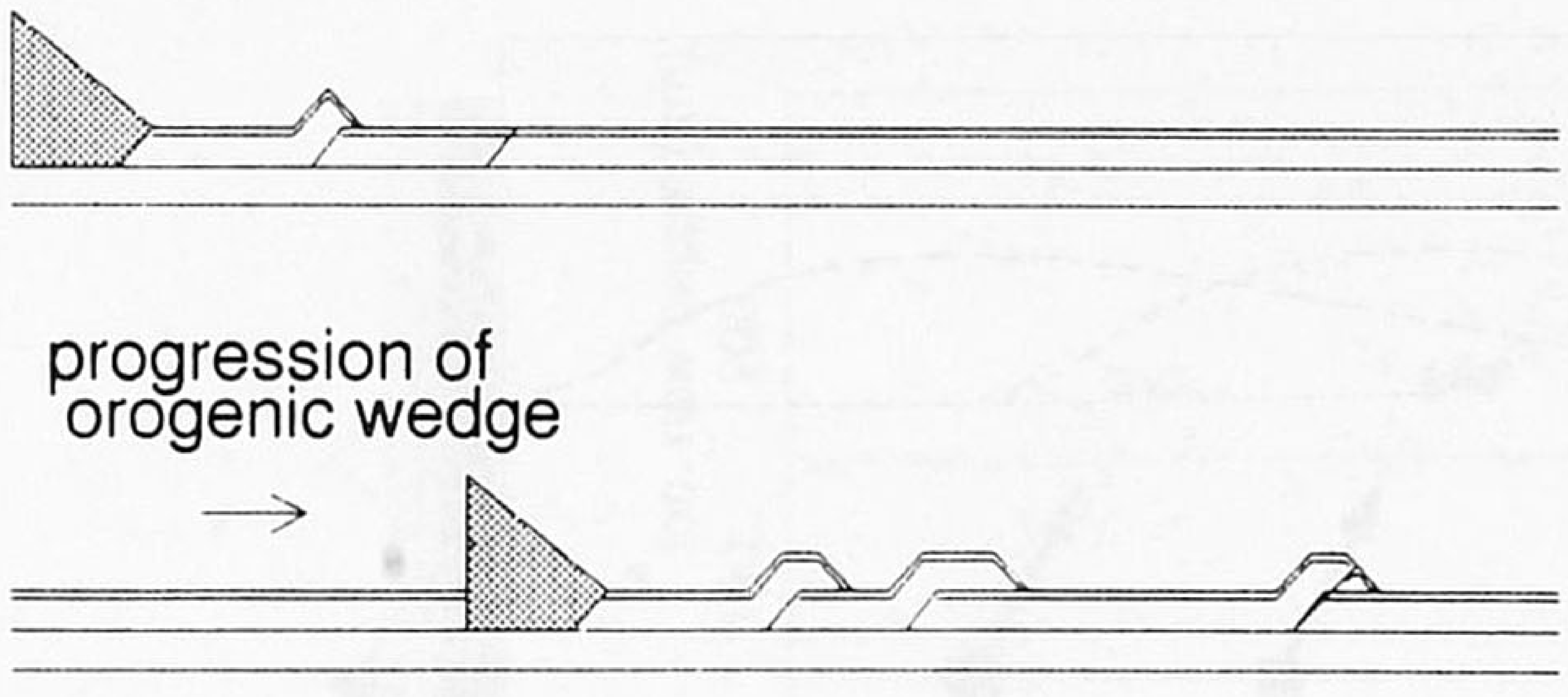

Figure 5. Effect of horizontal displacement of earlier emplaced loads on the shape of the wedge in the hinterland, when these loads are not replaced by new loads (see also text). The upper panel shows the initial configuration; the lower panel shows the situation after multiple thrust displacement.

fold-and-thrust belts (Silver *et al.* 1983; Mitchell 1984; Price 1986). Back thrusting is characterized by faults with movement towards the hinterland (Fig. 4e). Nappes prograde in the opposite direction of the general accretionary wedge movement, and may cut older nappes. We adopt 12.5 km for the thrust displacement and 25 km for the thrust spacing, which are consistent with observations (e.g. Silver & Reed 1988). The wedges are successively emplaced towards the hinterland.

Effects of thrusting on basin geometry

Fig. 6 shows the effect of the load width, without the incorporation of a failed rift, on the basin geometry. The vertical depth of locations at fixed distances from the wedge

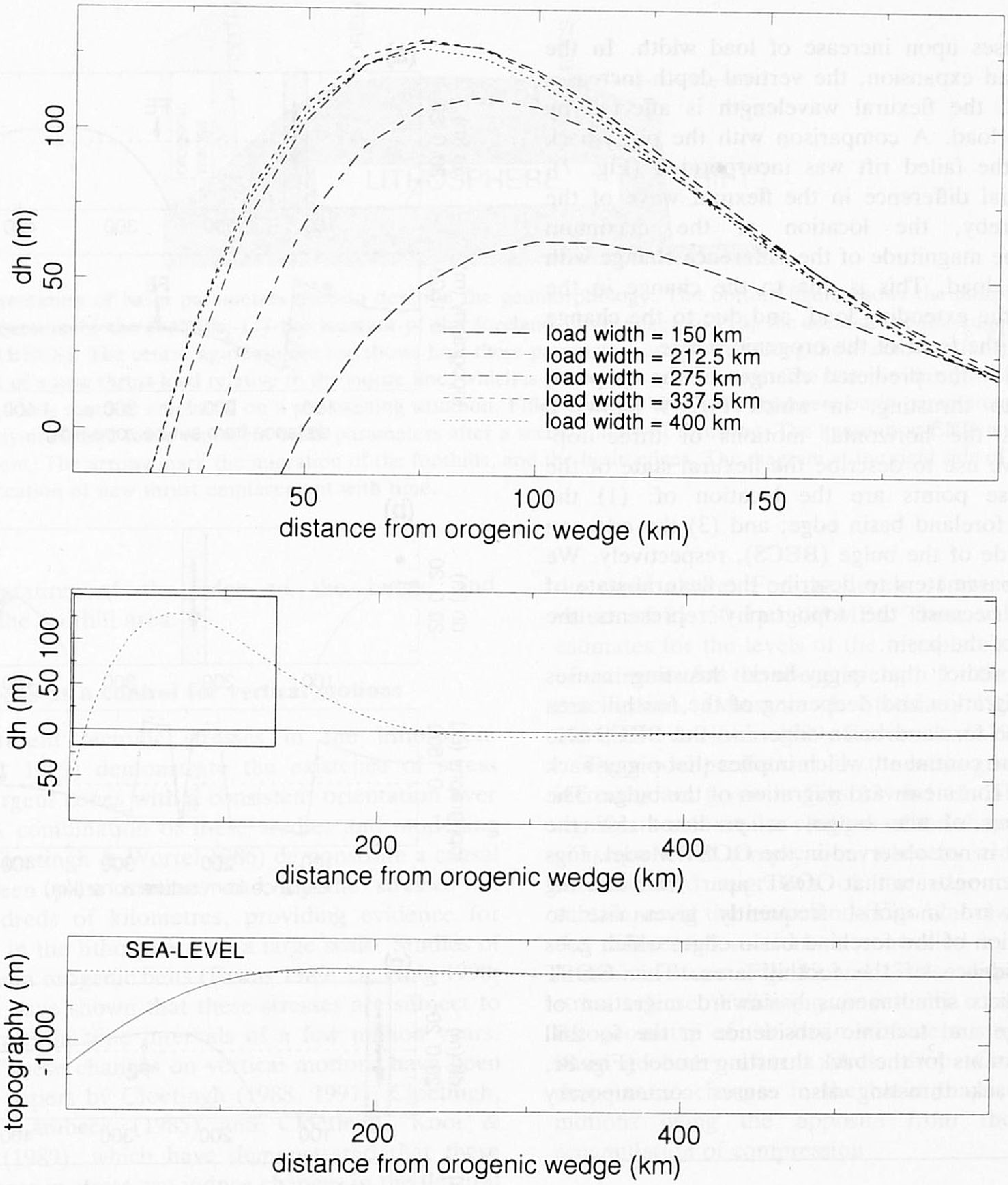

Figure 6. Effect of lateral extension of a wedge on the vertical height of the topography. Bottom: original topography; topography displayed as function of the distance to the front of the orogenic wedge. Centre: changes in height of the topography (*dh*) with an extension of the load width to 337.5 km. Top: detailed display of vertical changes due to extension of the load within distances of 150 km of the front of the wedge. In the first stage the bulge is uplifted and, consequently, the flexural wavelength of the lithosphere decreases, while in the latest stage the opposite changes occur.

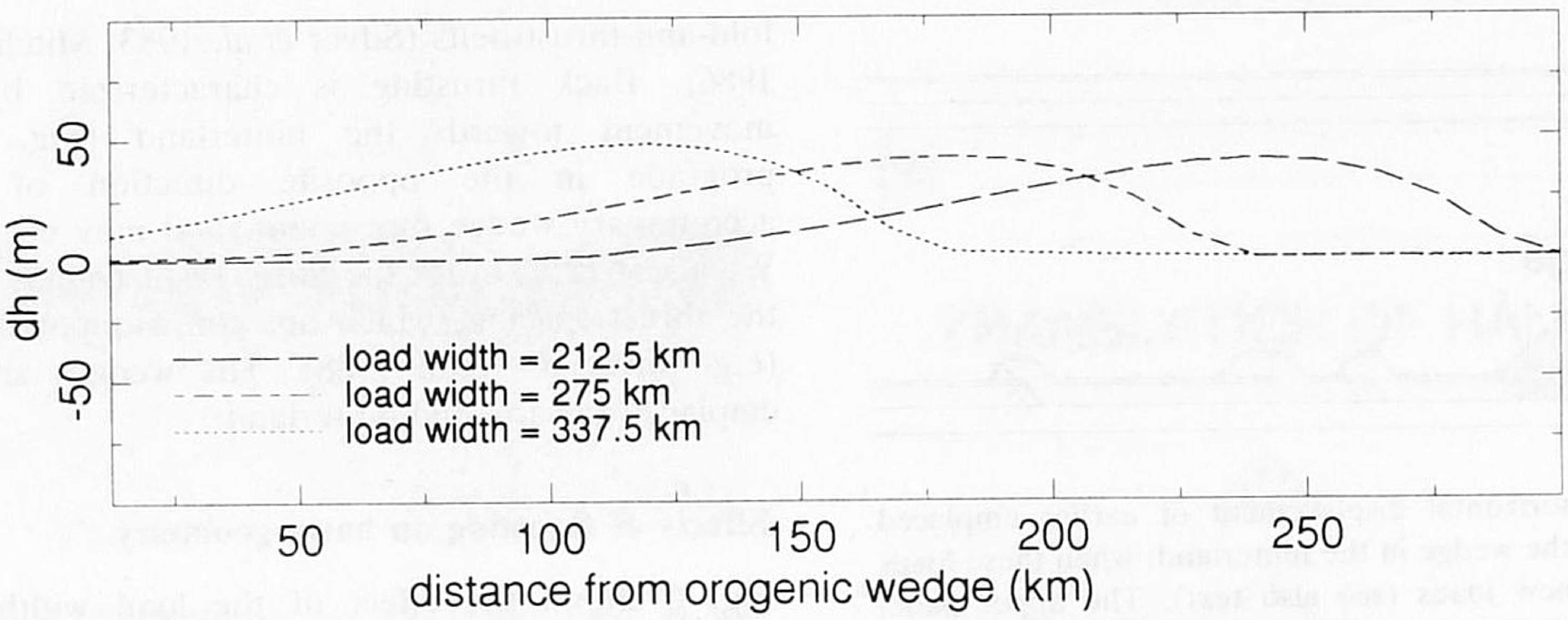

Figure 7. Changes of the topographic height (*dh*) as a consequence of the presence of a failed rift basin adjacent to the thrust loads. Figure shows the differences in basement height between piggy-back models with and without the incorporation of a failed rift. The location of maximum difference changes because the location of the front of the orogenic wedge changes.

drastically decreases upon increase of load width. In the latest stage of load expansion, the vertical depth increases again. Therefore, the flexural wavelength is affected by expansion of the load. A comparison with the piggy-back model whereby the failed rift was incorporated (Fig. 7), shows a substantial difference in the flexural wave of the lithosphere. Hereby, the location of the maximum difference, and the magnitude of the difference change with the width of the load. This is due to the change in the flexural wave of the extending load, and due to the change of the position of the front of the orogenic wedge.

Figs 8–10 display the predicted changes of the shape of the basin due to thrusting, in which Fig. 9 shows a representation of the horizontal motions of three topographic points we use to describe the flexural state of the lithosphere. These points are the location of: (1) the foothills; (2) the foreland basin edge; and (3) the edge on the continental side of the bulge (BECS), respectively. We use topographic parameters to describe the flexural state of the lithosphere, because the topography represents the actual basement of the basin.

The models predict that piggy-back thrusting causes continentward migration and deepening of the foothill area (Fig. 8a,10a). The foreland basin edge and the BECS also migrate toward the continent, which implies that piggy-back thrusting leads to continentward migration of the bulge. The continuous motion of the bulge, as predicted for the piggy-back model is not observed in the OOST Model. Figs 8(b) and 10(b) demonstrate that OOST, apart from causing initial continentward motions, frequently gives rise to basinward migration of the foreland basin edge, which goes along with subsidence of the foothill area. This OOST model thus predicts simultaneous basinward migration of the foreland edge and tectonic subsidence in the foothill area. The same counts for the back thrusting model (Figs 8c, 10c), because back thrusting also causes contemporary

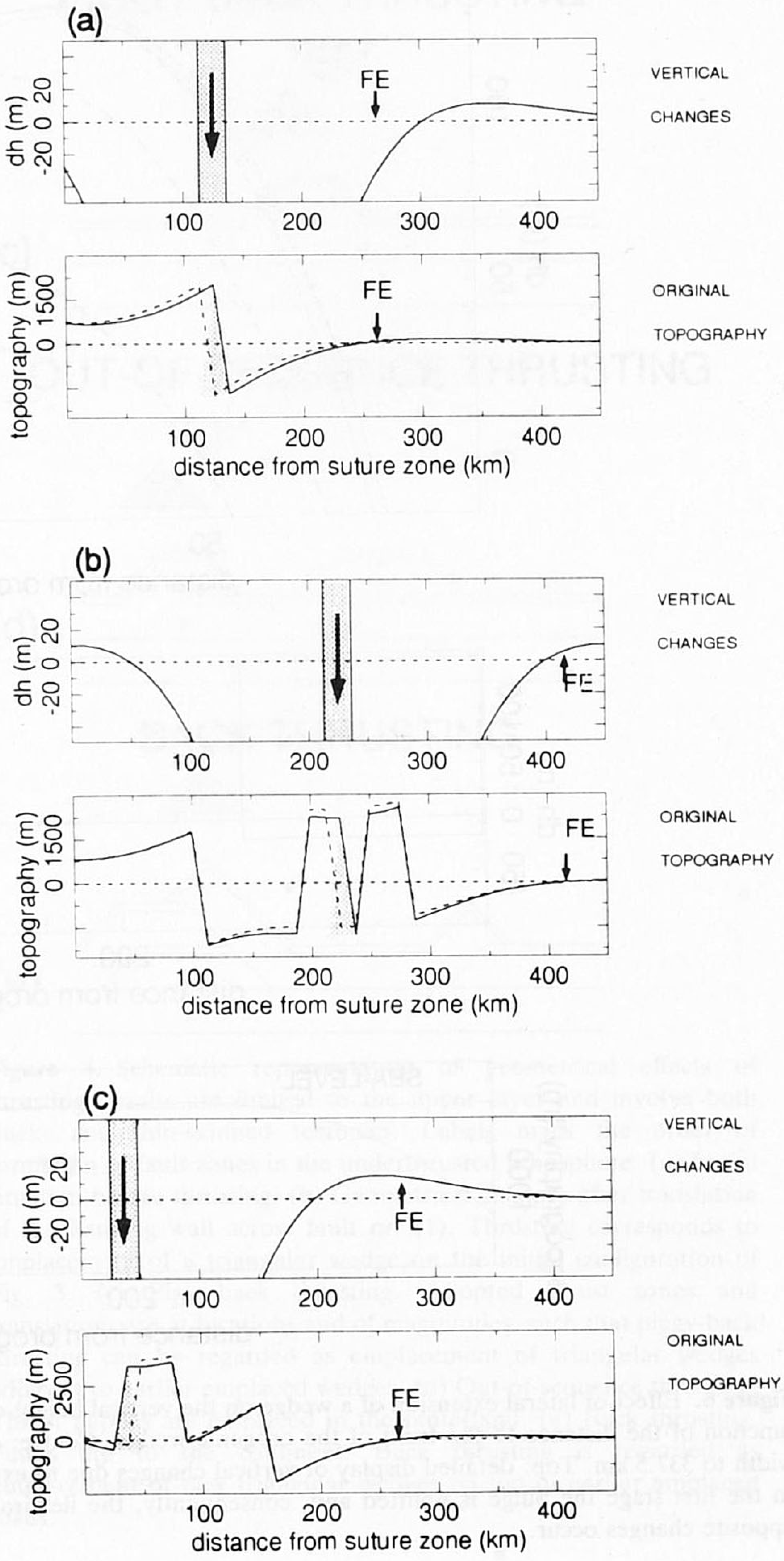

Figure 8. Examples of the effects of thrusting on the geometry of the basin with: (a) piggy-back thrusting; (b) out-of-sequence thrusting; and (c) back thrusting. Arrows in the shaded areas in the top figures mark the location of emplacement of a new load. The annotation FE marks the location of the foreland edge.

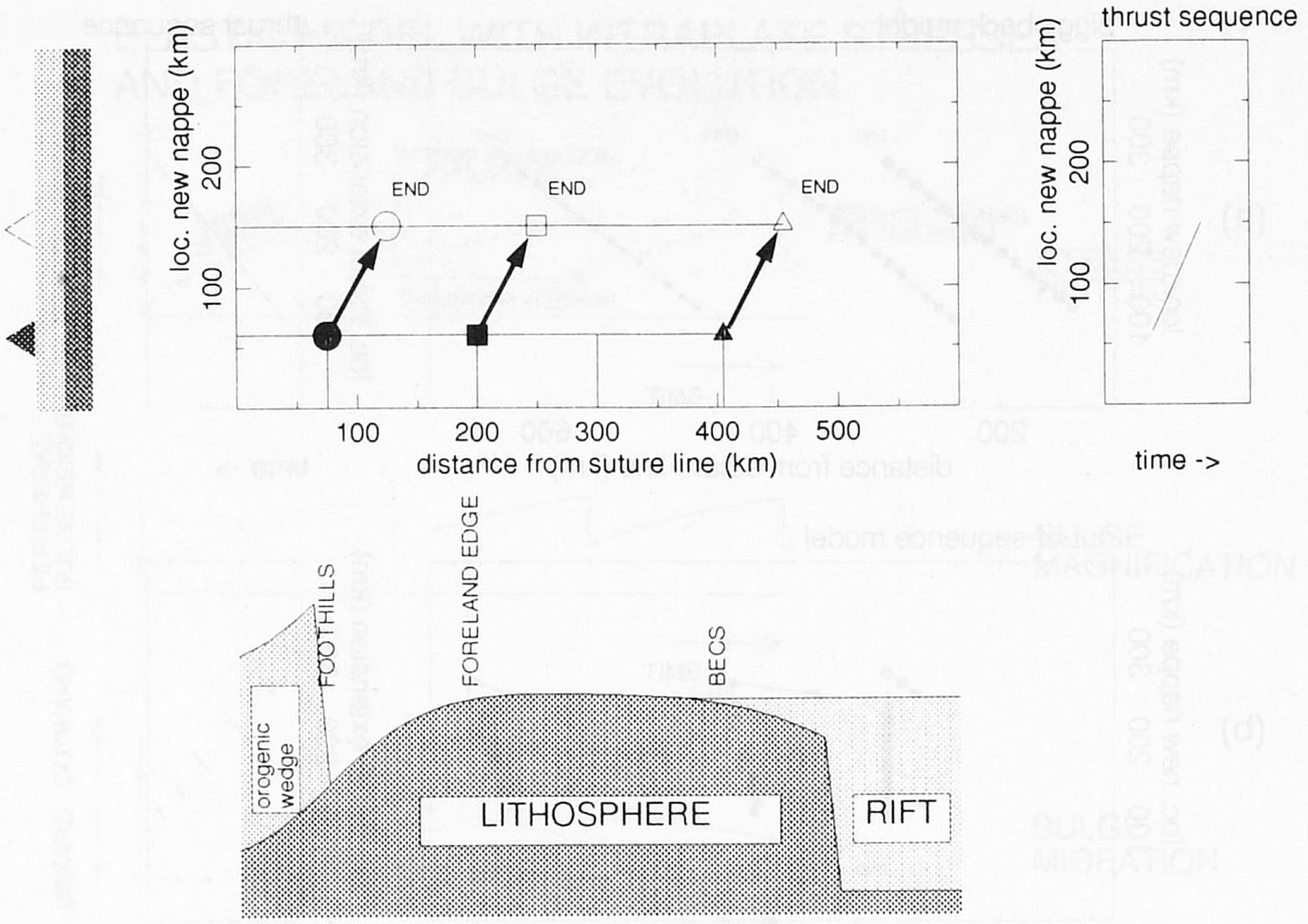

Figure 9. Representation of basin parameters used to describe the geomorphology. The bottom figure shows the morphology and the three points: (1) the location of the foothills; (2) the location of the foreland basin edge; and (3) the location of the edge of the bulge on the continental side (BECS). The centre figure on the top shows how these parameters are plotted along the x-axis, as a function of the location of the emplacement of a new thrust load relative to the suture line, which is plotted along the y-axis. The latter is illustrated with the left figure on the top, showing loads that are emplaced on a pre-existing situation. Filled symbols and loads represent basin parameters after a first phase of thrusting. Open symbols and loads represent basin parameters after a second phase of thrusting. The annotation END marks the final stage of thrust emplacement. The arrows mark the migration of the foothills, and the basin edges. The diagram at the right side of the figures shows the changes of the location of new thrust emplacement with time.

basinward migration of the edge of the bulge, and subsidence of the foothill area.

Stress fluctuations as a control for vertical motions

Studies of present tectonic stresses in the lithosphere (Zoback *et al.* 1989) demonstrate the existence of stress fields in convergent zones with a consistent orientation over large areas. A combination of these studies and modelling studies (e.g. Cloetingh & Wortel 1986) demonstrate a causal relation between plate motions and inplane stresses on scales of hundreds of kilometres, providing evidence for stress transfer in the lithosphere on a large scale. Studies of palaeo-stresses in orogenic belts (Evans 1989; De Ruig 1990; Mercier 1992) have shown that these stresses are subject to temporal changes in time intervals of a few million years. The effects of these changes on vertical motions have been elaborated in papers by Cloetingh (1988, 1991), Cloetingh, McQueen & Lambeck (1985) and Cloetingh, Kooi & Groenewoud (1989), which have demonstrated that these temporal changes in stress can induce changes in the flexural state of the lithosphere through time, and hence lateral motions of the flexural bulge (Fig. 11).

We have investigated the effect of intraplate stress fluctuations on the geometry of foreland basins, adopting the loading configurations used in the thrusting models discussed above. For the levels of the stresses we adopt values of 25, 50 and 100 MPa. These values are moderate estimates for the levels of the intraplate stress, also in view of estimates for the shear strength for thrust formation and reactivation, (Meissner & Strehlau, 1982; Dahlen *et al.* 1984; Ord & Hobbs 1989; Govers *et al.* 1992).

The model predictions for the basin geometry upon stress increases are given in Figs 12 and 13. The models predict significant and similar changes of the shape of the basin as a consequence of compression, whereby stress increase results in basinward migration of the edge of the bulge and subsidence of the hinterland (Figs 12a–c). The magnitude of the differential motions is controlled by the level of the horizontal stress. Figs 12 and 13 also display the effect of a stress release. Following an initially compressed situation, the geometry of the basin with zero stress represents the basin geometry after a stress drop. Consequently, stress drops cause changes in the basin shape, the directions of motions being the opposite from those in times of accumulation of compression.

Causes for differential vertical motions of the lithosphere

The models have shown that the shape of the basin depends on the width of the load. Furthermore, the difference of the piggy-back model and the OOST model demonstrates that

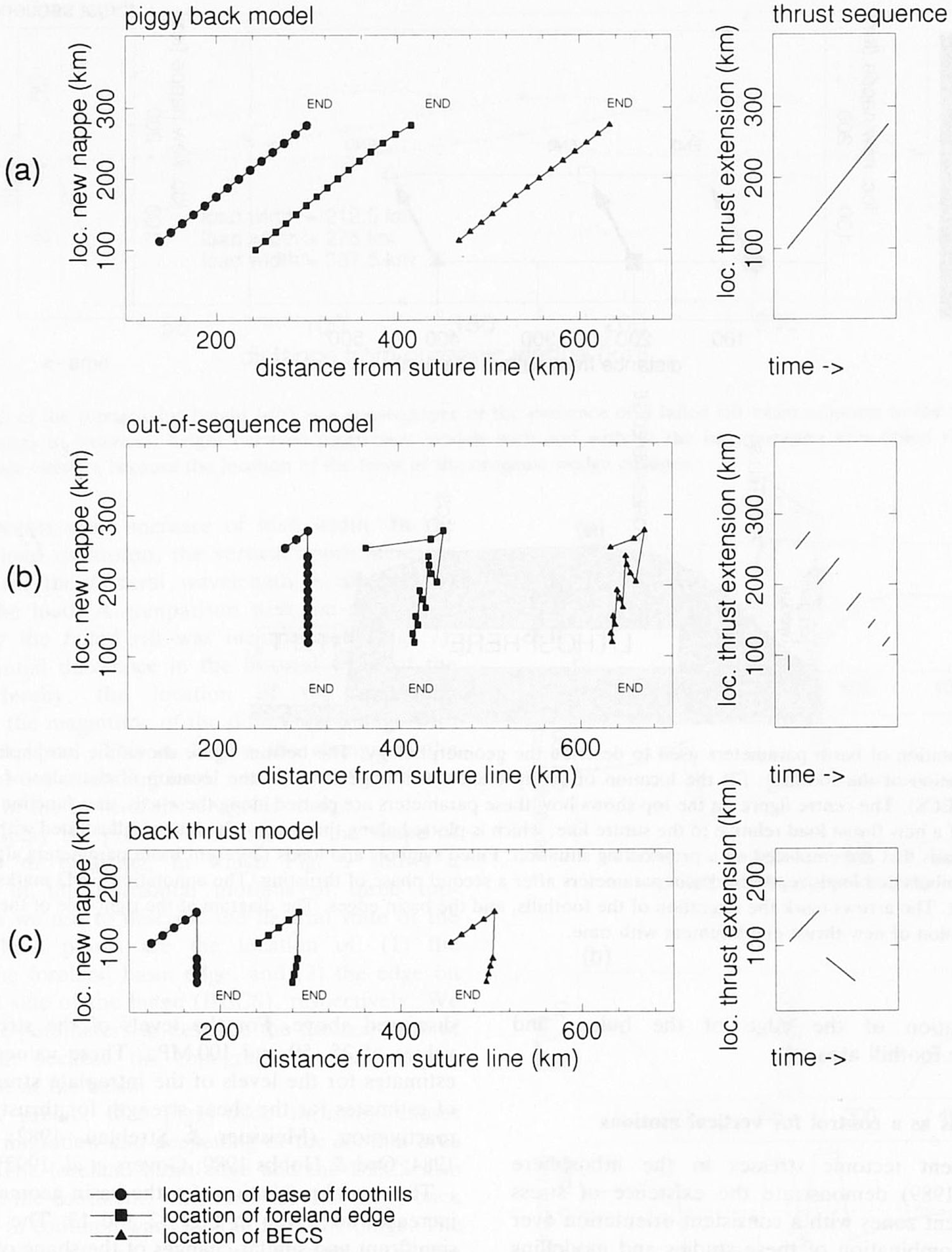

Figure 10. Changes of basin parameters as a consequence of thrust displacement with: (a) piggy-back thrusting; (b) OOST; and (c) back thrusting. Figure conventions as in Fig. 9.

not only the width of the load, but also the overall distribution of the load determines the ultimate shape of the basin. Changes of basin morphology are, therefore, partly the consequence of expanding the load, and partly the consequence of redistribution of the load. The effects are compatible with the effects of erosion and sedimentation. All these processes lead to changes of the load distribution with time.

The results of the piggy-back models demonstrate that the presence of a failed rift exerts an important control on the shape of the basin, as its flexural wave interferes with the flexural wave of the thrust load. The shape of the basin depends on the dominance of one of the flexural waves, which on its turn is determined by the shape and the volume of both the thrust loads and sedimentary infill of the rift basin. An example of the effects of a general dominance of the flexural wave of a displaced thrust load is given in Fig. 14, showing a foreland edge migration that is merely related to the migration of the flexural wave of the thrust load. The figure also shows, however, that the migration can temporarily be impeded, when the bulge of the static failed rift is dominant over the downward deflection related to the thrust load. The lateral dominance of each of the waves thus changes with thrust migration. Apart from this, the dominance changes with reorganizations of the geometry of the thrust load and the sedimentary basin. Such

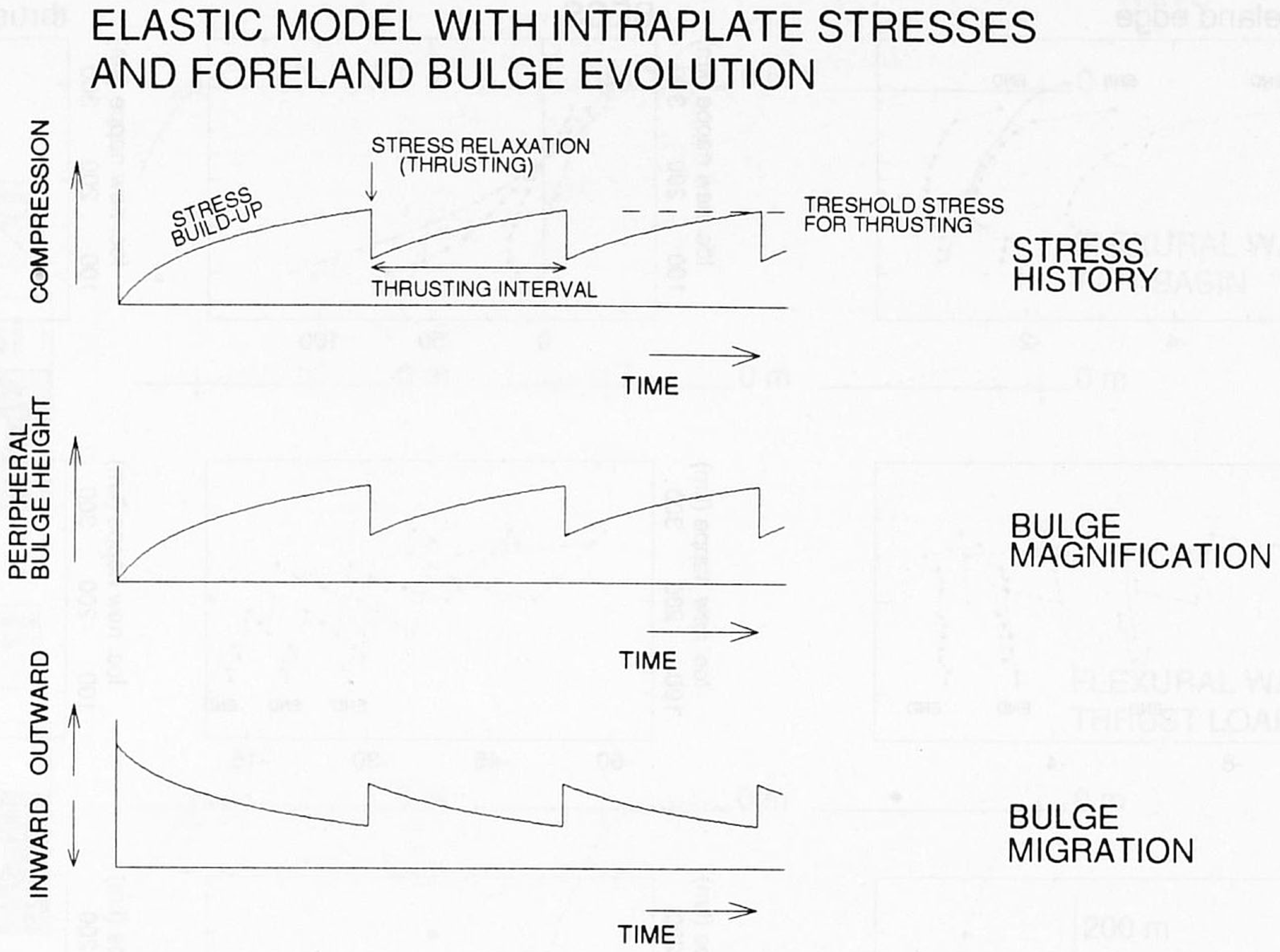

Figure 11. Model for changes in the flexural state of the lithosphere due to stress fluctuations and thrusting. Compressional stresses build up to a level at which the shear strength is exceeded and thrust displacement takes place, causing vertical and lateral differential motions of the bulge (after Cloetingh 1991).

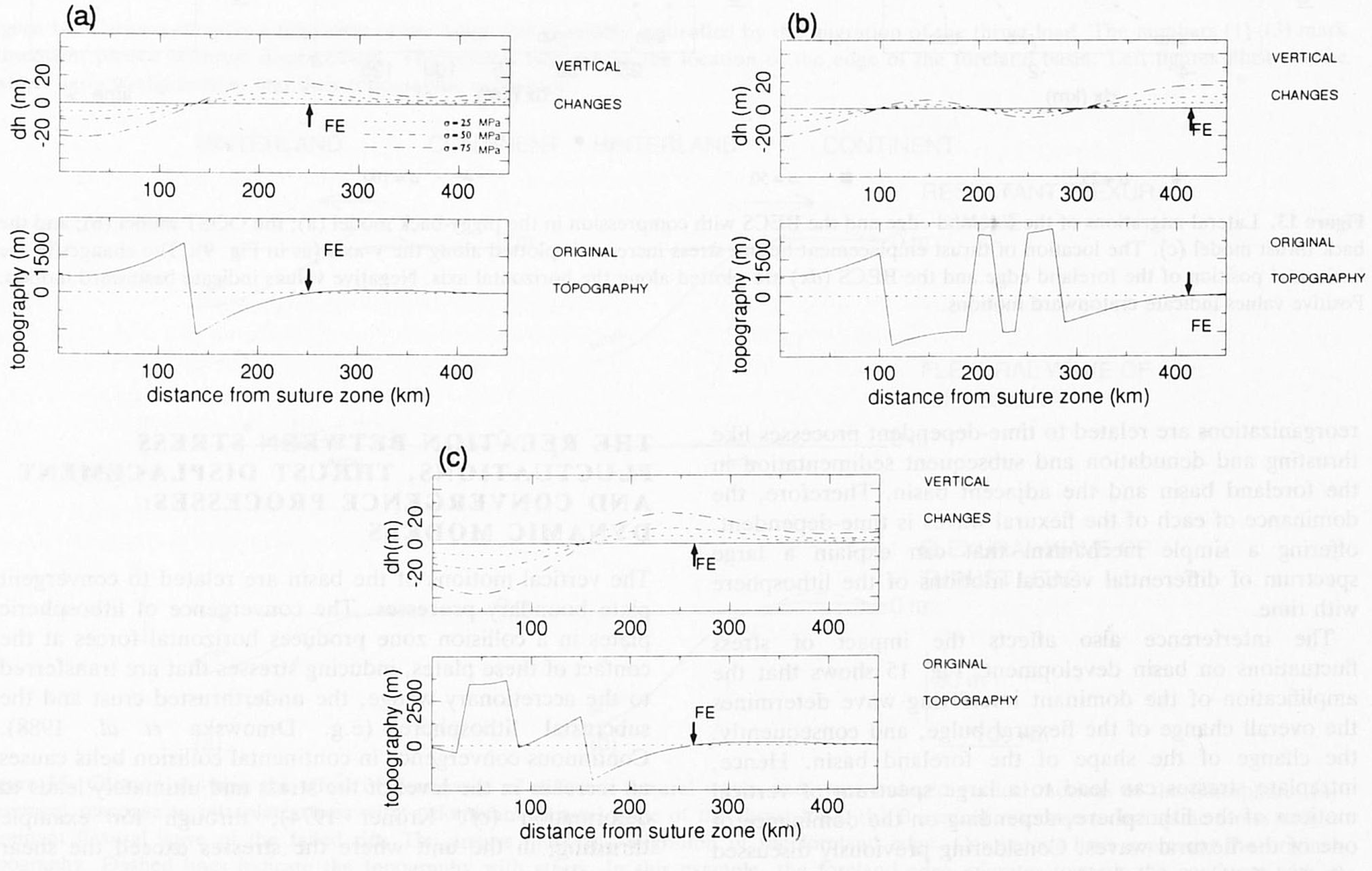

Figure 12. The effects of stress increase on the basin geometry for (a) the piggy-back model; (b) the out-of-sequence thrust model; and (c) the back thrust model. The annotation FE marks the location of the foreland edge.

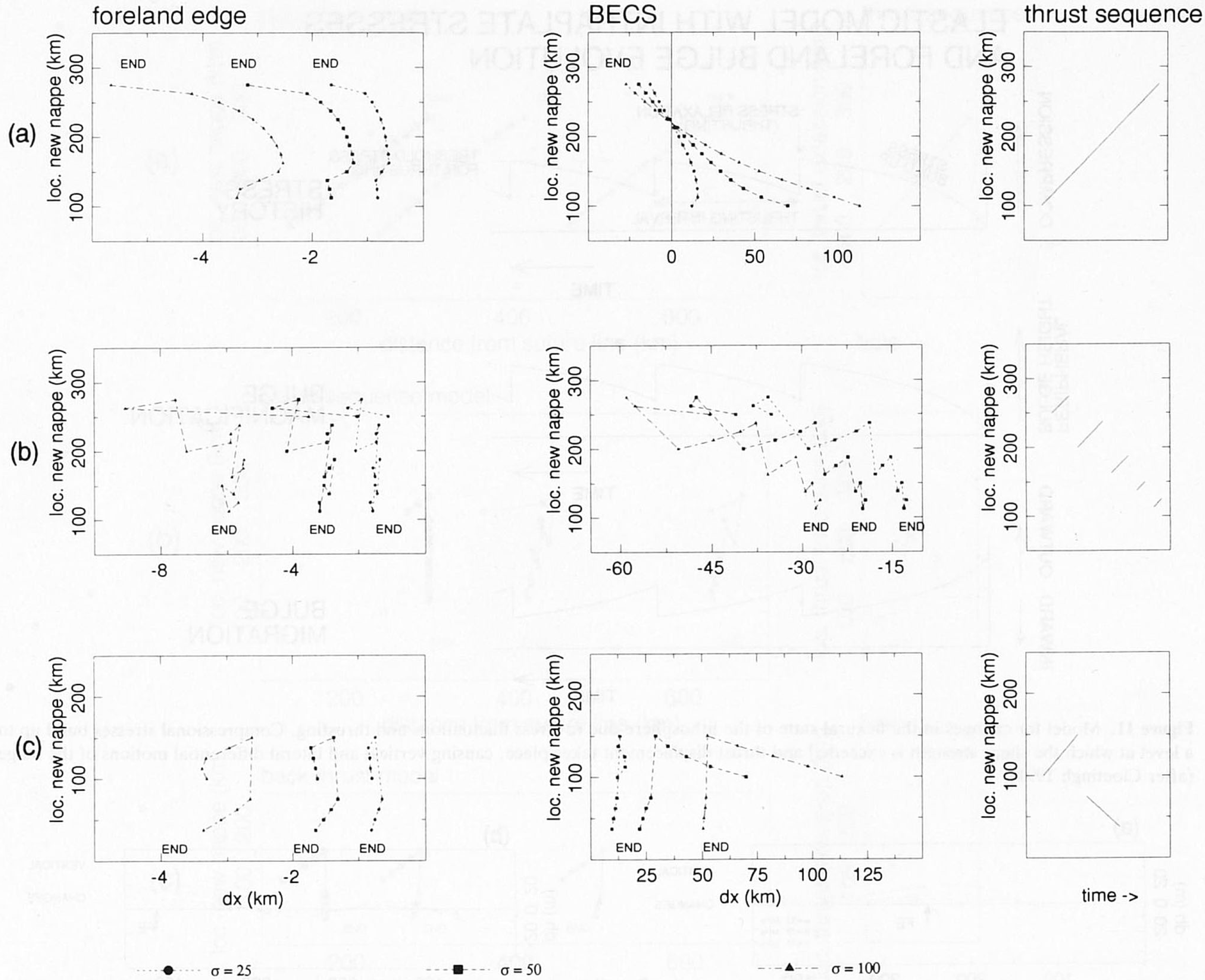

Figure 13. Lateral migrations of the foreland edge and the BECS with compression in the piggy-back model (a); the OOST model (b); and the back thrust model (c). The location of thrust emplacement before stress increase is plotted along the y-axis (as in Fig. 9). The changes in the horizontal position of the foreland edge and the BECS (dx) are plotted along the horizontal axis. Negative values indicate basinward motion. Positive values indicate cratonward motions.

reorganizations are related to time-dependent processes like thrusting and denudation and subsequent sedimentation in the foreland basin and the adjacent basin. Therefore, the dominance of each of the flexural waves is time-dependent, offering a simple mechanism that can explain a large spectrum of differential vertical motions of the lithosphere with time.

The interference also affects the impact of stress fluctuations on basin development. Fig. 15 shows that the amplification of the dominant interfering wave determines the overall change of the flexural bulge, and consequently, the change of the shape of the foreland basin. Hence, intraplate stresses can lead to a large spectrum of vertical motions of the lithosphere, depending on the dominance of one of the flexural waves. Considering previously discussed effects of changes of dominance with time, patterns of vertical motions due to stress also vary with time.

THE RELATION BETWEEN STRESS FLUCTUATIONS, THRUST DISPLACEMENT AND CONVERGENCE PROCESSES: DYNAMIC MODELS

The vertical motions of the basin are related to convergent plate boundary processes. The convergence of lithospheric plates in a collision zone produces horizontal forces at the contact of these plates, inducing stresses that are transferred to the accretionary wedge, the underthrusted crust and the subcrustal lithosphere (e.g. Dmowska *et al.* 1988). Continuous convergence in continental collision belts causes an increase in the level of the stress and ultimately leads to deformation (*cf*. Kröner 1974), through for example thrusting, in the unit where the stresses exceed the shear strength.

As shown in the previous section, the processes can lead

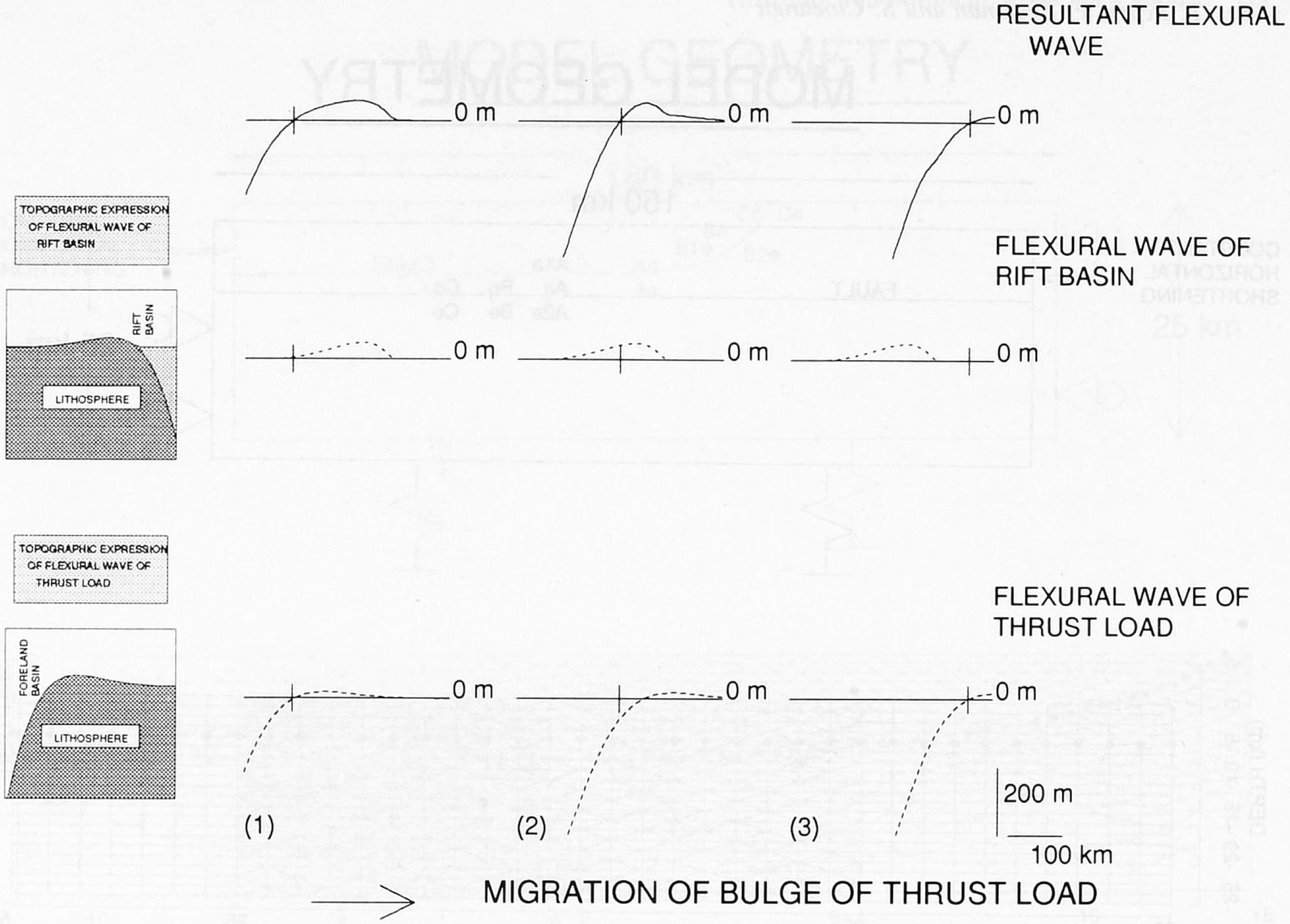

Figure 14. Cartoon showing a migration of the bulge that is mainly controlled by the migration of the thrust load. The numbers (1)–(3) mark subsequent phases of thrust displacement. The vertical bars marks the location of the edge of the foreland basin. Left figures illustrate the distinct basin configurations and their topographic expression.

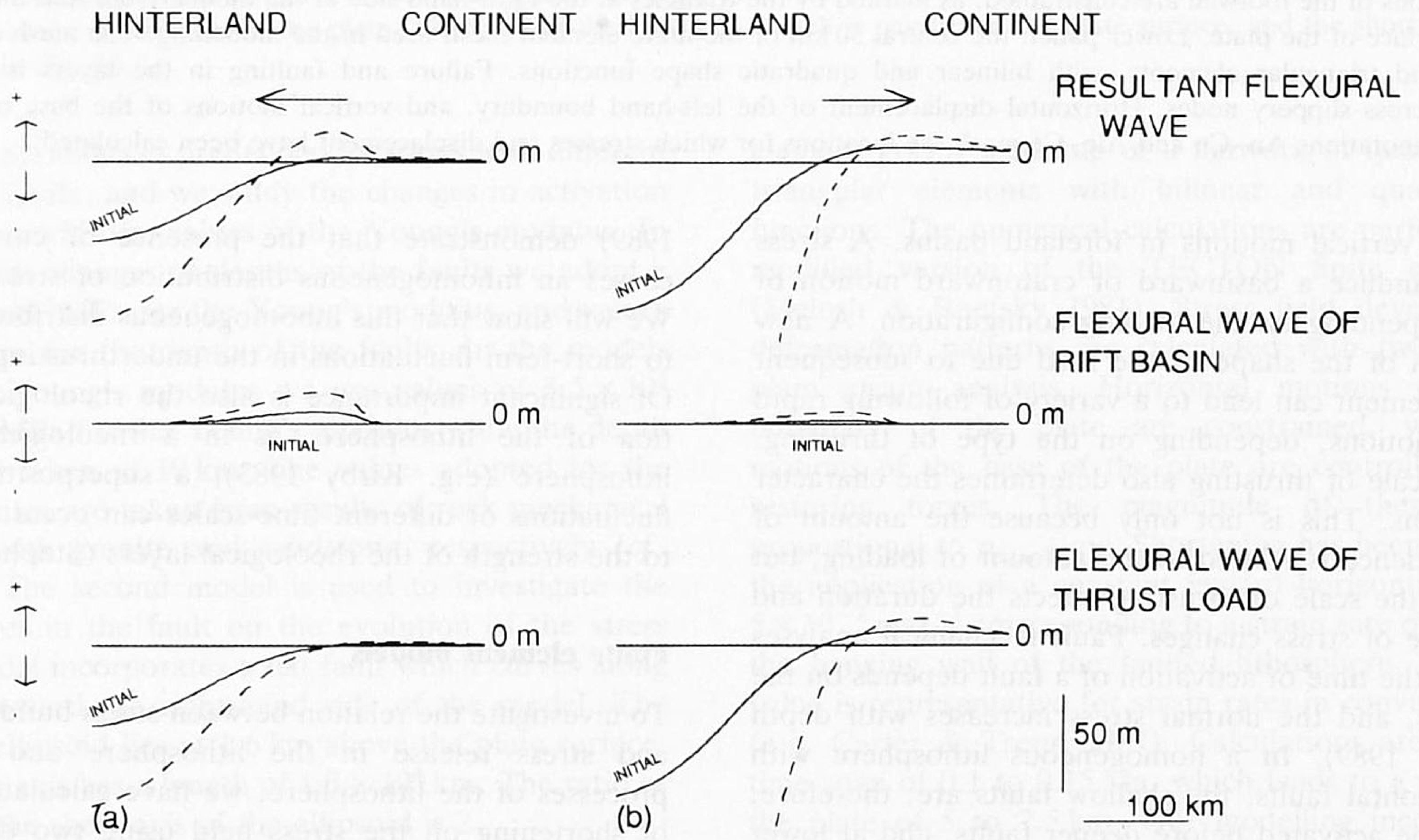

Figure 15. Cartoon showing the effect of dominance of different flexural waves and stress-induced vertical motions of the lithosphere. (a) Basement response to intraplate stress with a dominant flexural wave of the thrust load. (b) Basement response to intraplate stress with a dominant flexural wave of the failed rift. The arrows mark the migration of the foreland edge. Continuous lines represent the original topography. Dashed lines indicate the topography with stress. In this example, the foreland edge migrates towards the continent with a dominance of the deflection of the thrust nappes, while it migrates into the basin with a dominance of the deflection to the failed rift. Positive values indicate uplift, negative values indicate subsidence.

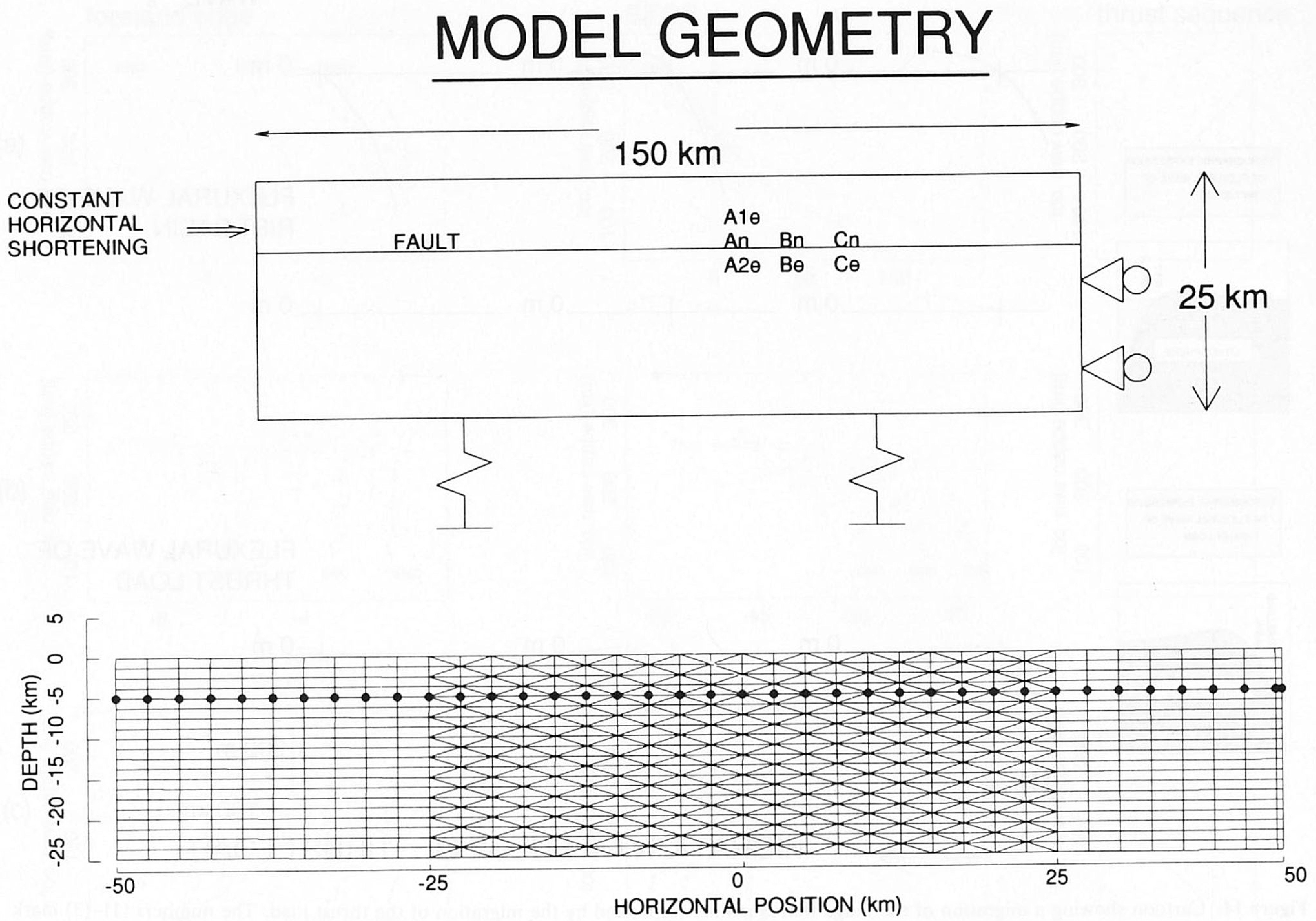

Figure 16. Upper panel: schematic representation of finite element model of a lithosphere with a flat fault. Faults have been modelled at depths of 5 and 10 km. Springs indicate isostatic restoring forces acting at the base of the lithosphere. Solid dots mark slippery nodes. The horizontal motions of the footwall are constrained, as marked by the triangles at the right-hand side of the model. Note that the fault does not reach to the surface of the plate. Lower panel: the central 50 km of the finite element mesh used in the modelling. The mesh consists of 1600 quadrilateral and triangular elements, with bilinear and quadratic shape functions. Failure and faulting in the layers is modelled with displacement across slippery nodes. Horizontal displacement of the left-hand boundary, and vertical motions of the base of the plate are constrained. Annotations An–Cn and Ale–Ce mark the locations for which stresses and displacement have been calculated.

to significant vertical motions in foreland basins. A stress increase can induce a basinward or cratonward motion of the bulge, depending on the loading configuration. A new reorganization of the shape of the load due to subsequent thrust displacement can lead to a variety of following rapid differential motions, depending on the type of thrusting. Herein, the scale of thrusting also determines the character of the motions. This is not only because the amount of flexural subsidence is related to the amount of loading, but also because the scale of thrusting affects the duration and the magnitude of stress changes. Fault mechanical analyses indicate that the time of activation of a fault depends on the normal stress, and the normal stress increases with depth (e.g. Ranalli 1989). In a homogeneous lithosphere with parallel horizontal faults, the shallow faults are, therefore, expected to be activated before deeper faults, and at lower stresses.

Another geometrical factor that can affect the duration of stress fluctuations is the shape of the faults. Both numerical and experimental models for stress distribution around inverted faults (e.g. Van Wees & Cloetingh 1991; McClay 1989) demonstrate that the presence of curves in faults causes an inhomogeneous distribution of stress and strain. We will show that this inhomogeneous distribution can lead to short-term fluctuations in the underthrusting lithosphere. Of significant importance is also the rheological configuration of the lithosphere, as in a rheologically stratified lithosphere (e.g. Kirby 1983), a superposition of stress fluctuations of different time-scales can occur, each related to the strength of the rheological layers (Stephenson 1989).

Finite element models

To investigate the relation between stress build up, thrusting and stress release in the lithosphere and convergence processes of the lithosphere, we have calculated the effects of shortening on the stress field using two different finite element models (Figs 16, 17 and Table 1). The first model is used to investigate the influence of the depth of the fault and the rheological properties on the time-scale of activation. This model incorporates flat horizontal faults only. We investigate the difference in time-scale for

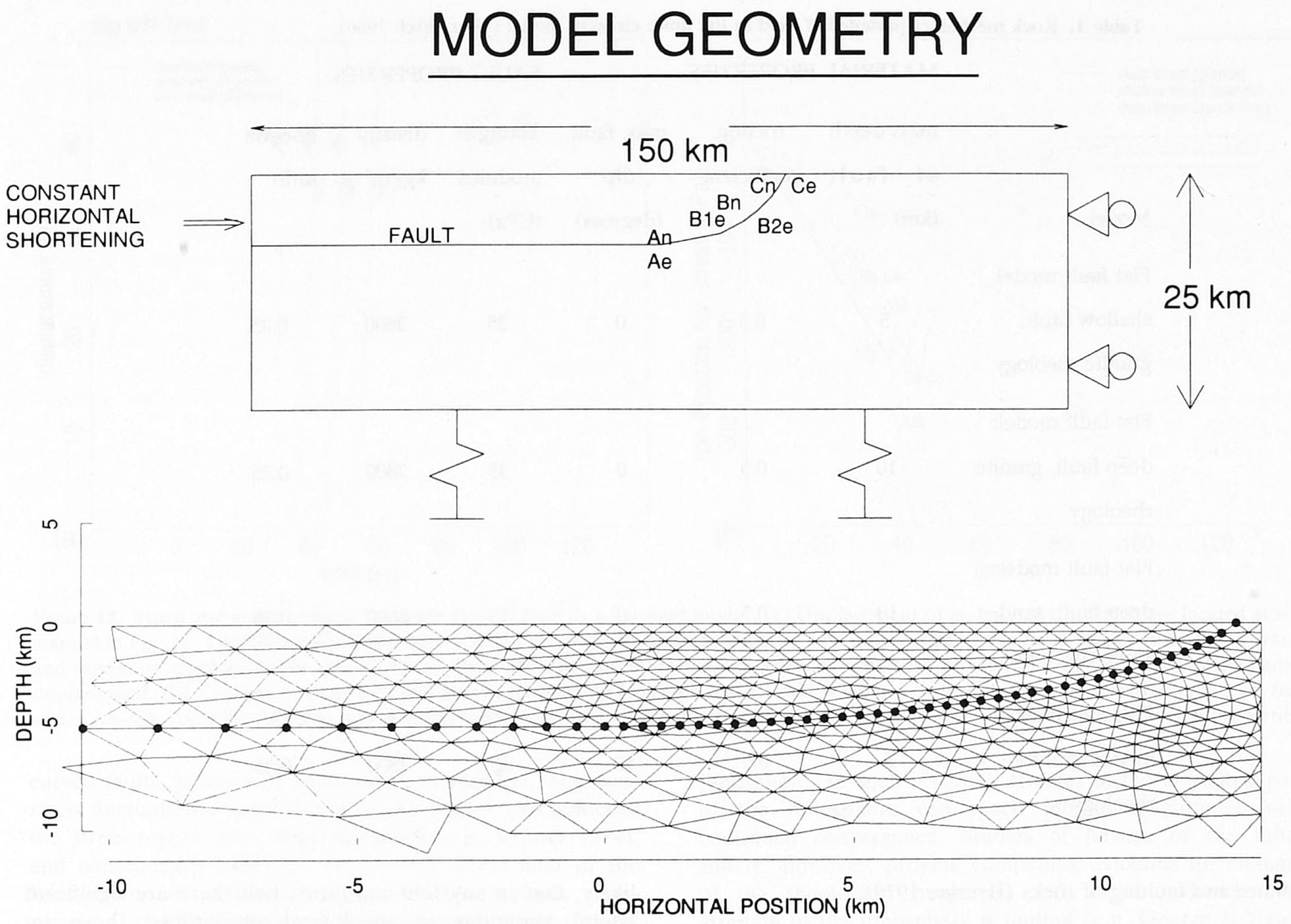

Figure 17. Upper panel: schematic representation of an ellipsoid fault model. Figure conventions as in Fig. 16. Note that the fault reaches the surface of the plate. The maximum depth of the fault is 5 km. Lower panel: the central 25 km of the mesh used in the modelling. The mesh consists of 1754 triangular elements, with bilinear and quadratic shape functions. The fault is defined by an ellipsoid with a focus point which lies at 1565 km above the surface of the plate. The ratio of the long axis, which is parallel to the plate surface, and the short axis is 2. Other conventions as in Fig. 16.

activation of slip nodes at predefined locations with different depths of the faults, and we study the changes in activation time in relation with the values of the Young's modulus. In the models with changes of depths of the faults we adopt a value of 3.5×10^4 MPa for the Young's modulus, and values of 5 and 10 km for the depth of the faults. In the models with variable Young's modulus we use values of 3.5×10^4 and 1.5×10^4 MPa for the Young's modulus while the depth of the fault is taken as 10 km. The values adopted for the Young's modulus are taken from results of rock mechanical experiments with granite and sandstone, respectively (*cf*. Birch 1966). The second model is used to investigate the effect of curves in the fault on the evolution of the stress field. The model incorporates a flat fault which curves along an ellipsoid toward the right-hand side of the model. The focus on the ellipsoid lies at 1.6 km above the plate surface, while the long axis has a length of 1.3×10^4 km. The ratio of the long and the short axis of the ellipsoid is 2.

In both the flat fault and the curved fault model we focus on the prime effects of thrust activation on the stress field, and therefore, ignore the effects of depth-dependent rheology on the magnitudes of the stress levels (e.g. Ranalli 1989), assigning elastic properties to the elements. The finite element grid is made up of a network of quadrilateral and triangular elements with bilinear and quadratic shape functions. The numerical calculations are performed with a modified version of the TECTON finite element code (Melosh & Raefsky 1981). Stress field development and deformation patterns are calculated with two-dimensional plain strain analysis. Horizontal motions of the right boundary of the plate are constrained, while vertical motions of the base of the plate are controlled by elastic restoring forces. The magnitude of these forces is proportional to $\rho_{\text{mantle}} g w$. Shortening has been modelled by the application of a constant inward horizontal velocity of 5×10^{-2} m yr^{-1} corresponding to a strain rate of 10^{-14} s^{-1} to the hanging wall of the faulted lithosphere. The adopted value is representative for strain rates in convergence zones (e.g. Carter & Tsenn 1987). Calculations are made for a time span of 0.1 to 0.15 Ma, which leads to a shortening of the plate of 5 to 7.5 km. Our modelling incorporates the effects of faulting in the layers, by the introduction of an algorithm for slippery nodes (*cf*. Melosh & Raefsky 1981). Friction across the faults has also been taken into account, adopting Amonton's law for reactivation of faults (equation 3, Ranalli 1989), and experimental laboratory data on

Table 1. Rock mechanics parameters used in the finite element model (after Birch 1966).

	MATERIAL PROPERTIES			FAULT PROPERTIES		
Model	max. depth of fault (km)	friction coefficient	max. fault dip (degrees)	Young's modulus (GPa)	density kg/m³	Poisson ratio
Flat fault model: shallow fault, granite rheology	5	0.5	0	35	2800	0.25
Flat fault model: deep fault, granite rheology	10	0.5	0	35	2800	0.25
Flat fault model: deep fault, sandstone rheology	10	0.5	0	15	2800	0.25
Ellipsoid fault model, granite rheology	5	0.5	30	35	2800	0.25

failure and faulting of rocks (Byerlee 1978).

$$|\tau| = \mu_0 \sigma_n, \tag{3}$$

where τ is the shear stress, μ_0 is the coefficient of friction, and σ_n is the normal stress acting on the fault plane. For the friction coefficients we adopted a value of 0.5. The maximum fault dip in the curved fault models is 30°. For reasons of convenience, we ignore the effects of irregularities of fault planes and fault annealing (e.g. Sibson 1986; Stel 1986) on the stress–strain evolution of the faults.

Stress accumulation with time

Fig. 18 shows the predictions for local and temporal timing of thrust activation and changes of the non-lithostatic horizontal stress at points at fixed distances from the faults, in the flat fault models. The figures show that equivalent slippery nodes in the shallow fault are approximately 10 000 yr earlier displaced than nodes in the deeper fault model. Fig. 18(b) shows that the later activation takes place at higher stress levels, which confirms views discussed in the previous section. The predicted increase of 40 000 yr of the activation time with a lower Young's modulus (Fig. 18a) illustrates the importance of the rheology for the time-scales of stress changes. These predictions can be explained by the higher strain that can be taken up by the lithosphere with the smaller Young's modulus. The models confirm that stress changes in the lithosphere depend on the scale of thrusting, and the rheological properties.

These findings have important implications for the evolution of the stress regime in fold-and-thrust belts. It is likely, that in any fold-and-thrust belt there are significant lateral variations in rheological properties. These inhomogeneities can act as accumulation points for stress (Schedl & Wiltschko 1987; Van Wees & Cloetingh 1991), which we refer to as stress ramps. Continuous strain leads, in this situation, to a build up of an inhomogene stress field. Ultimately, collapse occurs at the ramp and a non-uniform change of the stress field is induced. Therefore, both temporal stress build ups and relaxations, and thus fluctuations can be generated. As a result, resembling stress ramps at different depths initiate different types of stress fluctuations. Deep ramps generate longer term higher magnitude fluctuations than shallow ramps. Similarly, different rheological inhogeneities at similar depths generate different stress fluctuations.

In the foregoing we focused on the effects of lateral inhomogeneities in rock composition, but lateral variations in rheological properties are not the only inhomogeneities that cause accumulations of stress. As mentioned before, faults can also generate inhomogeneous stress fields and can thus also act as stress ramps. Fig. 19 displays the results for the curved fault model, and shows that the stress and strain patterns in time become significantly more complicated than with a simple flat fault. Stress fluctuations are predicted, which are related to significant changes in the displacement rate. The presence of a curve in a fault thus induces local, temporal fluctuations. Inspection of Figs 18 and 19 indicates that the curve of faults significantly controls the duration and the magnitude of stress fluctuations. Highly curved faults form greater stress ramps, and therefore, generate longer term higher amplitude stress fluctuations than lesser

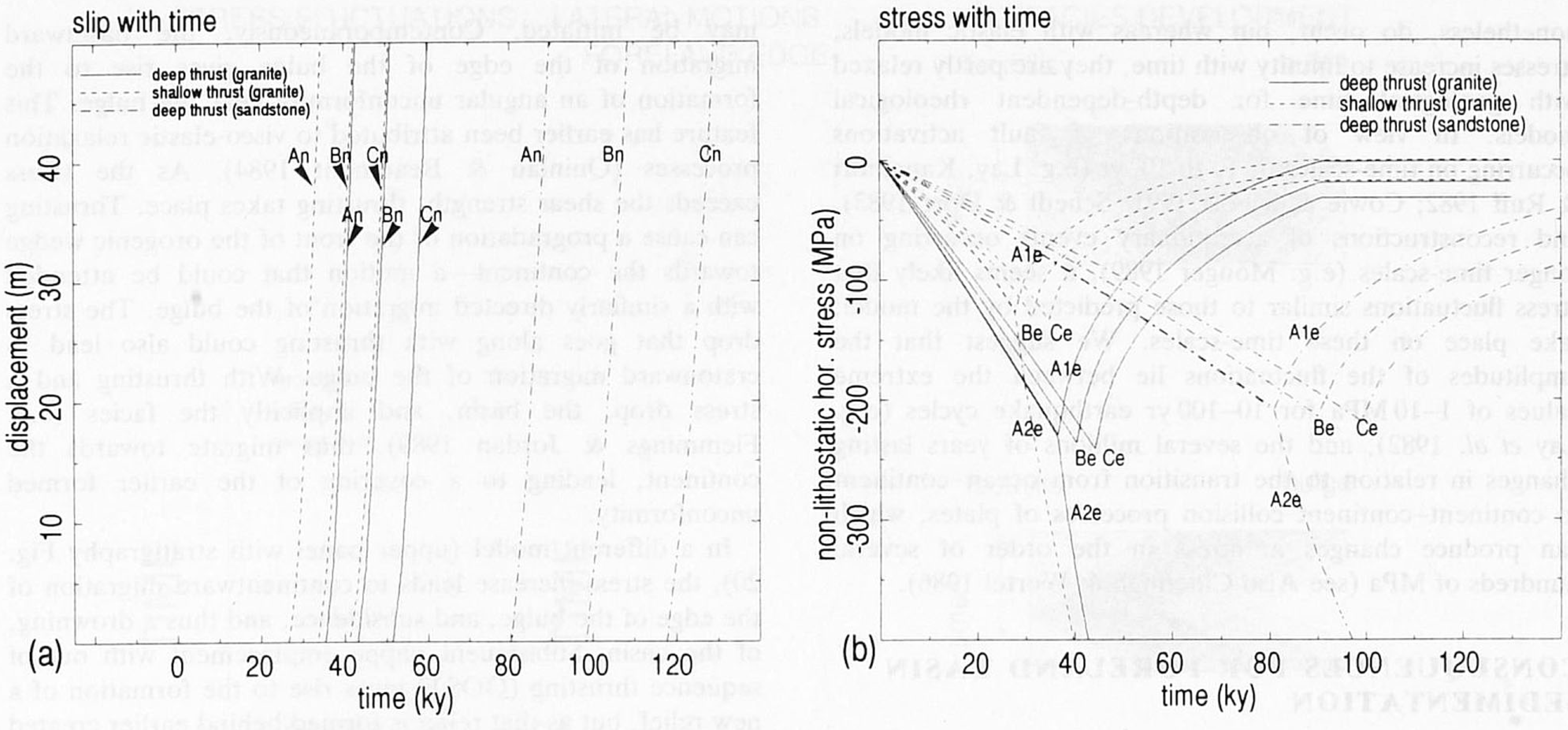

Figure 18. Stress and strain at fixed locations along a fault in a flat-fault model. (a) Displacement of nodes An–Cn, which are located at sites marked in Fig. 16. The differently drawn curves reflect the displacement of the nodes with different depths of faults (5 and 10 km), and granite and sandstone rheologies (see also Table 1). Note that the nodes located closest to be shortened boundary in the model, undergo earliest displacement. (b) Changes of non-lithostatic horizontal stress at locations A1e–Ce which lie at a vertical distance of approximately 2 km from nodes An–Cn. As in the different curves reflect model predictions for models with different depth of faults and different rheological properties.

curved faults, in cases of horizontal compression. The local stress fluctuations, as predicted by the model, can influence the stress regime over large distances (e.g. Kröner 1974), and consequently influence the overall stress field of the lithosphere. As a result, changes in the tectonic stress regime of the lithosphere are the integrated effects of local stress fluctuations.

The local stress fluctuations are in the order of 50 MPa in 40 000 yr, but are calculated for an elastic model of the lithosphere. In such a model, stresses in the unfaulted part of the lithosphere can reach infinite magnitudes with continued convergence. Studies of flexure of the lithosphere, however, provide compelling evidence for changes of the rheological properties with depth, whereby the strength of the lithosphere is limited (e.g. Goetze & Evans 1979). This implies that the magnitude and the duration of stress accumulation in the lithosphere is limited. Fluctations of the stress level, as predicted by the elastic model

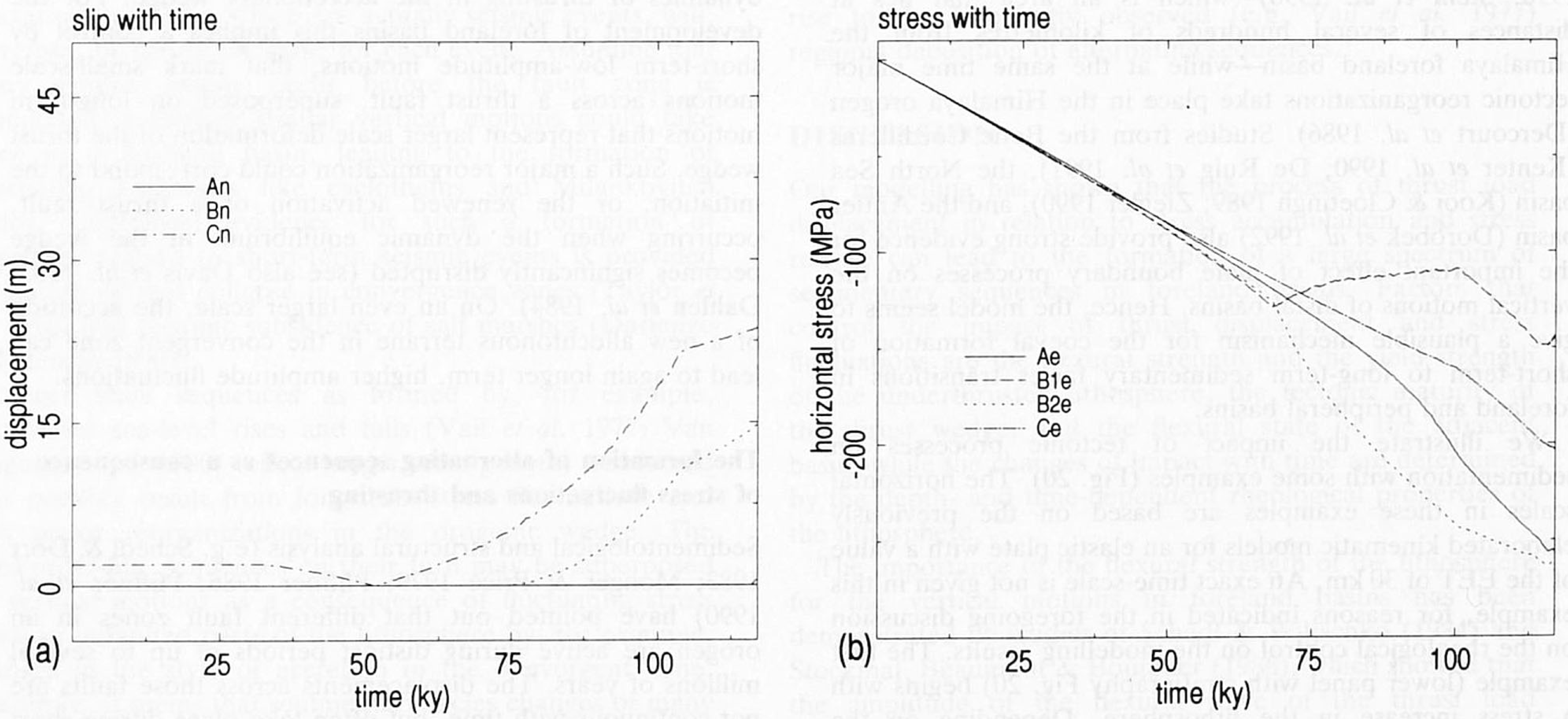

Figure 19. Stress and strain at fixed locations along a fault in an ellipsoid fault model. (a) Displacement of nodes An–Cn. The curves reflect an irregular pattern of displacement with time between 80 000 to 115 000 yr. (b) Changes of non-lithostatic horizontal stress at locations Ae–Ce which lie at a vertical distance of approximately 1 km from nodes An–Cn. The irregular displacement influences the stress field between 80 000 and 115 000 yr, and a non-uniform stress change with time occurs.

nonetheless, do occur, but whereas with elastic models, stresses increase to infinity with time, they are partly relaxed with geological time for depth-dependent rheological models. In view of observations of fault activations occurring on time-scales of 10 to 10^6 yr (e.g. Lay, Kanamori & Ruff 1982; Cowie & Scholz 1991; Schedl & Dorr 1983), and reconstructions of accretionary events occurring on longer time-scales (e.g. Monger 1989), it seems likely that stress fluctuations similar to those predicted by the model, take place on these time-scales. We suggest that the amplitudes of the fluctuations lie between the extreme values of 1–10 MPa for 10–100 yr earthquake cycles (e.g. Lay *et al.* 1982), and the several millions of years lasting changes in relation to the transition from ocean–continent to continent–continent collision processes of plates, which can produce changes in stress in the order of several hundreds of MPa (see Also Cloetingh & Wortel 1986).

CONSEQUENCES FOR FORELAND BASIN SEDIMENTATION

The combined results of the finite element models and the previously described kinematic models point to a large spectrum of predicted vertical motions in foreland basins with time. Studies of subsidence and facies patterns have shown that facies development is strongly controlled by tectonically induced vertical motions (e.g. Embry 1989; Nemec 1988; Kenter *et al.* 1990; Peper & Cloetingh 1992) and, therefore, the mechanism also gives a new explanation for a number of observations of facies changes in foreland basins. Furthermore, the stress fluctuations can be transferred over large distances (Stephenson & Cloetingh 1991; Ziegler 1990; Zoback *et al.* 1989) affecting vertical motions in adjacent areas. Studies from plate motions and corresponding facies transitions have shown significant vertical motions in the northeastern Indian Ocean (Cochran 1990; Stein *et al.* 1990)—which is an area that lies at distances of several hundreds of kilometres from the Himalaya foreland basin—while at the same time major tectonic reorganizations take place in the Himalaya orogen (Dercourt *et al.* 1986). Studies from the Betic Cordilleras (Kenter *et al.* 1990; De Ruig *et al.* 1991), the North Sea basin (Kooi & Cloetingh 1989; Ziegler 1990), and the Antler basin (Dorobek *et al.* 1992) also provide strong evidence for the important effect of plate boundary processes on the vertical motions of distal basins. Hence, the model seems to give a plausible mechanism for the coeval formation of short-term to long-term sedimentary facies transitions in foreland and peripheral basins.

We illustrate the impact of tectonic processes on sedimentation with some examples (Fig. 20). The horizontal scales in these examples are based on the previously elaborated kinematic models for an elastic plate with a value of the EET of 30 km. An exact time-scale is not given in this example, for reasons indicated in the foregoing discussion on the rheological control on the modelling results. The first example (lower panel with stratigraphy Fig. 20) begins with a stress increase in the lithosphere. Depending on the loading geometry, the stress increase leads to the basinward migration of the edge of the bulge and subsidence of the nappes in the foothill area. Since the nappes subside and the relief thus has decreased, a marine inundation of the area may be initiated. Contemporaneously, the basinward migration of the edge of the bulge gives rise to the formation of an angular unconformity near the bulge. This feature has earlier been attributed to visco-elastic relaxation processes (Quinlan & Beaumont 1984). As the stress exceeds the shear strength, thrusting takes place. Thrusting can cause a progradation of the front of the orogenic wedge towards the continent—a motion that could be attended with a similarly directed migration of the bulge. The stress drop that goes along with thrusting could also lead to cratonward migration of the bulge. With thrusting and a stress drop, the basin, and implicitly the facies (e.g. Flemmings & Jordan 1989), thus migrate towards the continent, leading to a covering of the earlier formed unconformity.

In a different model (upper panel with stratigraphy Fig. 20), the stress increase leads to continentward migration of the edge of the bulge, and subsidence, and thus a drowning, of the basin. Subsequent nappe emplacement with out of sequence thrusting (OOST) gives rise to the formation of a new relief, but as that relief is formed behind earlier created topography, and at a large distance from the basin, thrusting would probably not lead to basinward progradation of a coarse clastic wedge. On the contrary, thrusting could be attended with simultaneous subsidence of the foothills, and basinward migration of the bulge. This process induces an overall drowning of the basin, which is interrupted by the formation of an erosional unconformity at and around the bulge. Such features have been observed in the Mississippian stratigraphy of the Appalachian foreland basin (Craig & Varnes 1979; De Witt & McGrew 1979).

In the model, the time-scale of the transitions of sedimentary facies corresponds to the time-scale of the stress fluctuations. We have shown that these fluctuations could be related to thrust events, and it is, therefore, likely that the duration of vertical motions is controlled by the dynamics of thrusting in the accretionary wedge. For the development of foreland basins this implies a control by short-term low-amplitude motions, that mark small-scale motions across a thrust fault, superposed on long-term motions that represent larger scale deformation of the thrust wedge. Such a major reorganization could correspond to the initiation, or the renewed activation of a thrust fault, occurring when the dynamic equilibrium in the wedge becomes significantly disrupted (see also Davis *et al.* 1983; Dahlen *et al.* 1984). On an even larger scale, the accretion of a new allochtonous terrane in the convergent zone can lead to again longer term, higher amplitude fluctuations.

The formation of alternating sequences as a consequence of stress fluctuations and thrusting

Sedimentological and structural analysis (e.g. Schedl & Dorr 1983; Monger & Price 1979; Pfiffner 1986; Pfiffner *et al.* 1990) have pointed out that different fault zones in an orogen are active during distinct periods of up to several millions of years. The displacements across those faults are not continuous with time, but often take place during short subsequent phases, whereby the fault displacements are in the order of some metres per event (e.g. De Bremaecker 1987). This implies that the changes in the loading redistribution on terms of hundreds to thousands of years

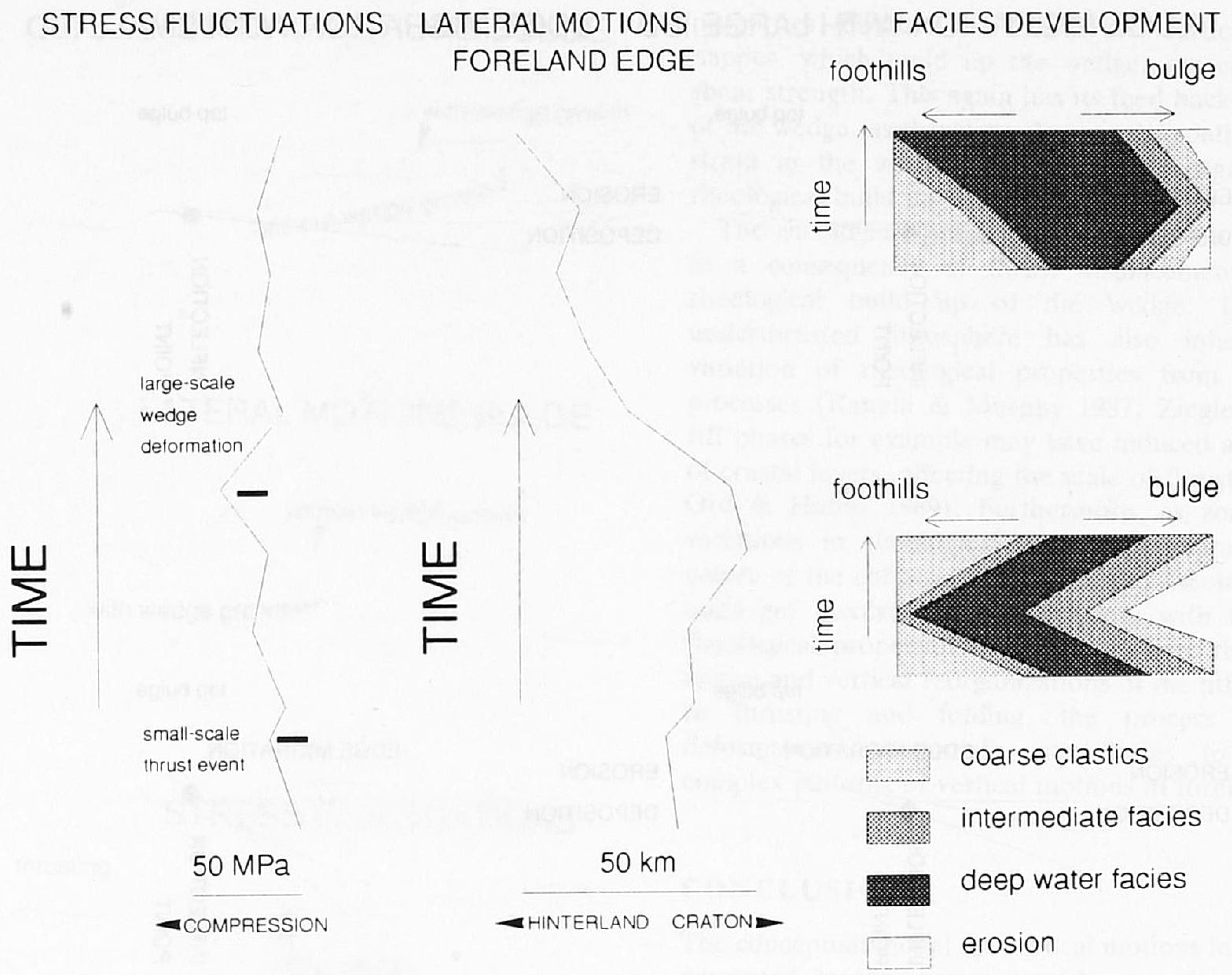

Figure 20. Changes of sedimentary facies with time as a consequence of stress increase, thrusting and stress relaxation (see also text). Left figure shows the changes in the state of stress of the lithosphere. Middle figure shows how the foreland edge may migrate due to these stress fluctuations. Lower right figure shows how the sedimentary facies can migrate basinward due to stress increase, while they migrate cratonward with subsequent thrusting. Upper right figure illustrates how a stress increase can cause a regional drowning of the basin, while subsequent thrusting results in a basinward migration of the bulge attended with a hinterlandward migration of the deep water facies. The adopted scales are based on kinematic elastic models, discussed in the text.

are negligible. The effects of stress increases and subsequent relaxation processes, which are actually seismic events, will, therefore, be nearly the same for each event. Assuming that many seismic events occur before the fault zone is abandoned, repetitive similar vertical motions could take place in a foreland basin, leading to the formation of alternating sequences like cyclothems and Milankovitch cycles. Geological evidence for such a formation of sequences related to short-term seismic events is provided by studies of reef collapse in convergence zones (Taylor *et al.* 1990) and tectonic subsidence of salt marshes (Darienzo & Peterson 1990).

Larger scale sequences as formed by, for example, third-order sea-level rises and falls (Vail *et al.* 1977; Van Wagoner *et al.* 1990) reflect longer term general trends and thus possibly result from long-term stress fluctuations and thus major reorganizations in the orogenic wedge. The third-order-like sequences on their turn may be superposed on vertical motions as a consequence of fluctuating stress levels in unfaulted parts of the lithosphere by, for example, changes in the style of accretion in the convergent zone. Therefore, it seems that sedimentary facies changes of many different time-scales in foreland basins can be the result of intraplate stress fluctuations and thrust movements. In view of the previously discussed regional effect of stress fluctuations in adjacent areas, the short-term and long-term vertical motions can also occur in peripheral basins, giving rise to the frequently observed (e.g. Vail *et al.* 1977) regional deposition of alternating sequences.

DISCUSSION

Our modelling has shown that the process of thrust load displacement in relation to stress accumulation and stress release can lead to the formation of a large spectrum of sedimentary sequences in foreland basins. Factors that control the impact of thrust displacement and stress fluctuations are the flexural strength and the yield strength of the underthrusted lithosphere, the tectonic maturity of the thrust wedge, and the flexural state of the adjacent basin, while the changes of impact with time are determined by the depth- and time-dependent rheological properties of the lithosphere.

The importance of the flexural strength of the lithosphere for the vertical motions in foreland basins has been demonstrated by studies of Schedl & Wiltschko (1984) and Stockmal, Beaumont & Boutelier (1986), which showed that the amplitude of the flexural wave of the thrust load significantly increases, while the wavelength of the flexural wave of the thrust load decreases, with a decrease of the EET. Consequently, the magnitude of the vertical motions due to stress increase and thrusting in foreland basins

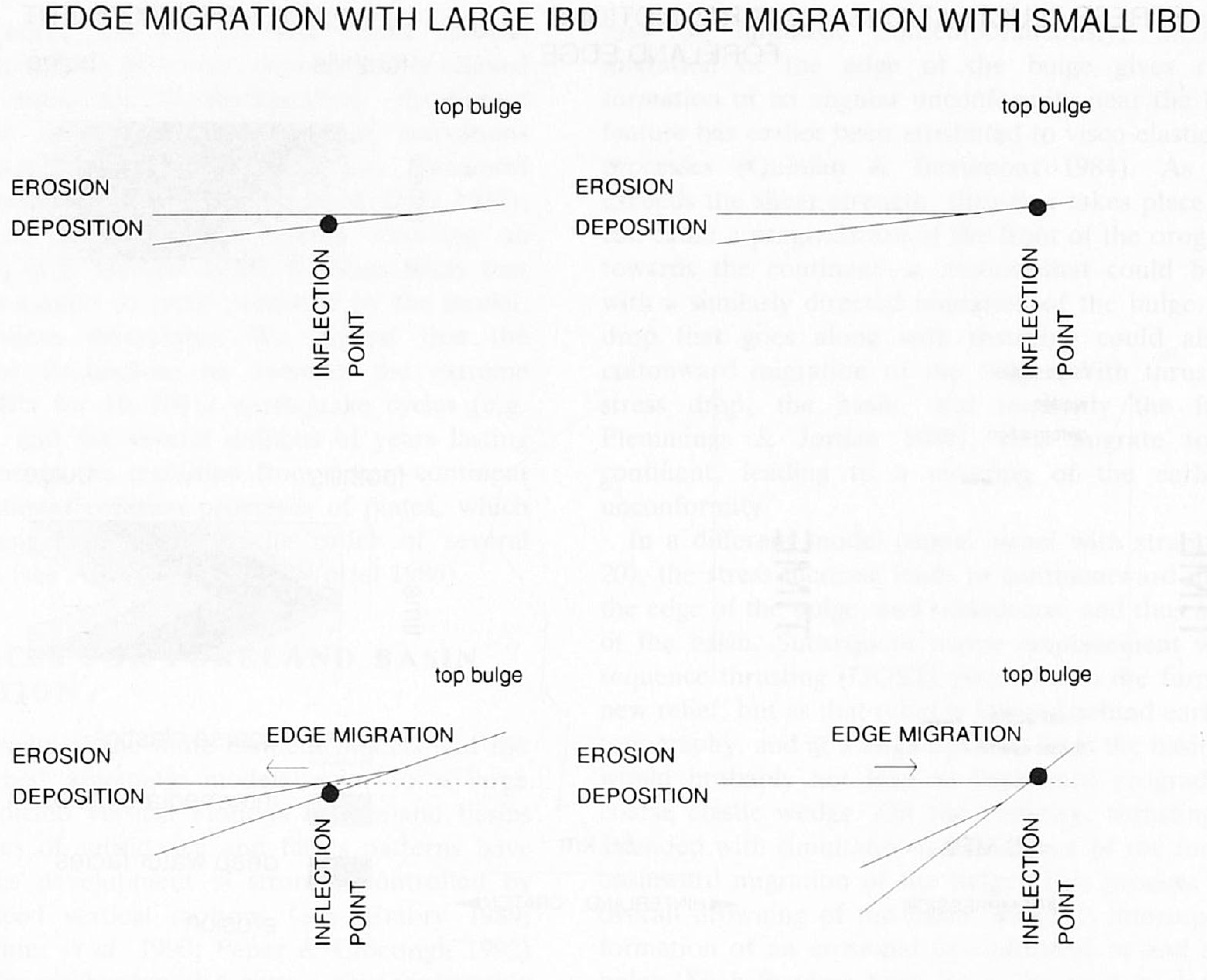

Figure 21. Changes in the migration of the foreland edge related to the difference between the distance between the inflection point and the bulge (IBD) with a large EET (left column) and a small EET (right column). Note the difference in sedimentation patterns.

located on a relatively weak lithosphere will be larger. This does not only mean that facies changes can be more dramatic, but also that the migration direction of facies patterns can be completely different, as the horizontal and vertical distances from the inflection point to the top of the bulge (IBD = inflection point – bulge distance) are smaller. Stress accumulation that would produce basinward motions of the foreland edge with a large IBD could produce cratonward motions with a small IBD (Fig. 21). In this respect, results of studies of intraplate deformation of continental lithosphere, which have demonstrated the substantial influence of depth-dependent rheology of the folding characteristics of the lithosphere (Stephenson & Cloetingh 1991; Cloetingh 1991; Fig. 22) are of particular importance. Vertical motions with depth-dependent models compared to vertical motions with elastic models, are of a larger magnitude, which implies that smaller stress fluctuations are sufficient to cause significant vertical motions. Furthermore, the models have different IBDs and consequently the direction of bulge migration can be influenced.

Apart from the flexural strength of the lithosphere, the tectonic maturity of the accretionary wedge also controls the impact of stress fluctuations and thrust displacement on facies development. In an immature thrust wedge for which the thickness is doubled by imbricate thrusting, the impact of thrust emplacement will be much more dramatic than the impact of a similar displacement in a mature wedge, which only implies a small magnification of the volume. In contrast

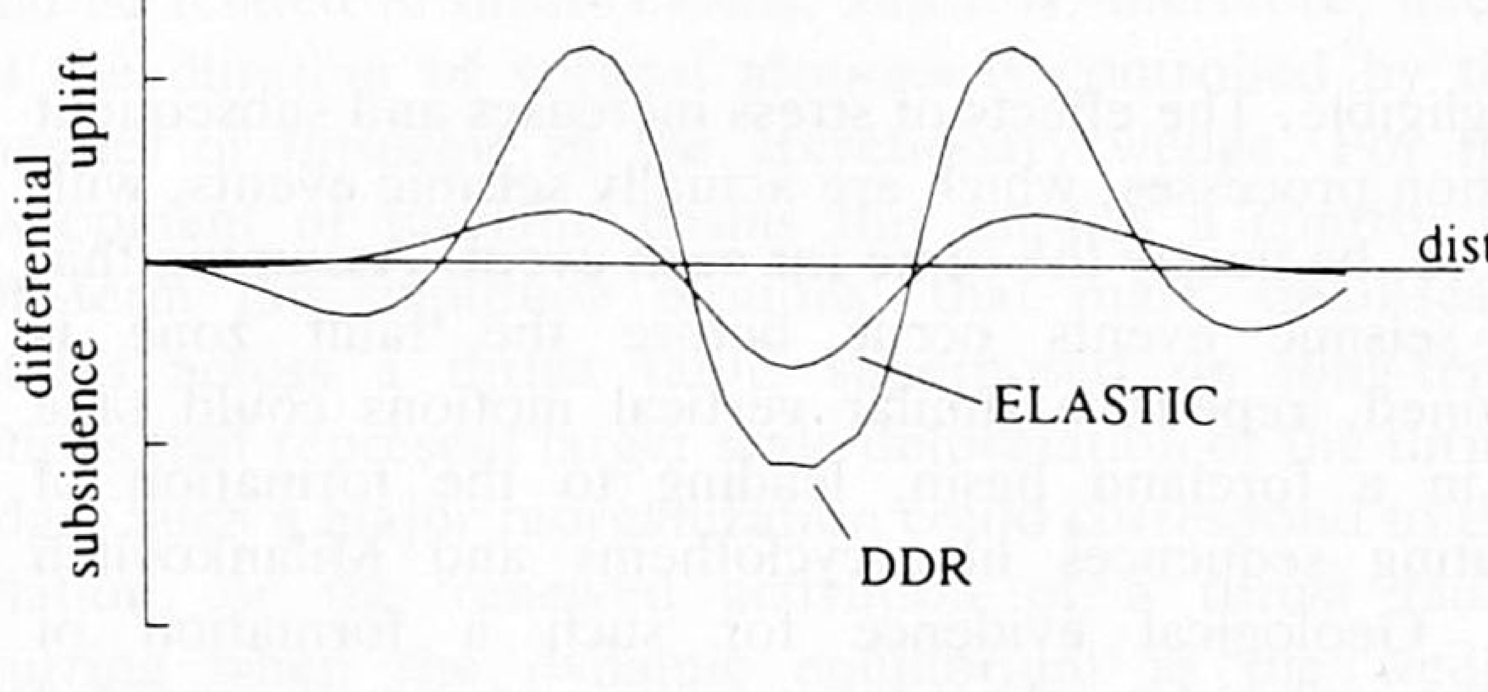

Figure 22. Comparison of compression induced differential subsidence and uplift of the lithosphere with depth-dependent rheology (DDR) and elastic rheology (after Cloetingh 1991).

with this, the impact of the stress fluctuations upon tectonic maturity will be larger, because the magnification factor of the deflection as a consequence of stress remains the same (Hetenyi 1946). Differential vertical motions due to stress thus increase with the volume of the load. Therefore, our model implies that the character of the vertical motions changes with the tectonic maturity of the orogenic belt. Vertical motions, and implicitly facies transitions, due to thrusting in relatively mature orogens become less important, while flexural changes due to stress increase will become of increasing significance (Fig. 23).

Furthermore, where the effect of intraplate stress on the

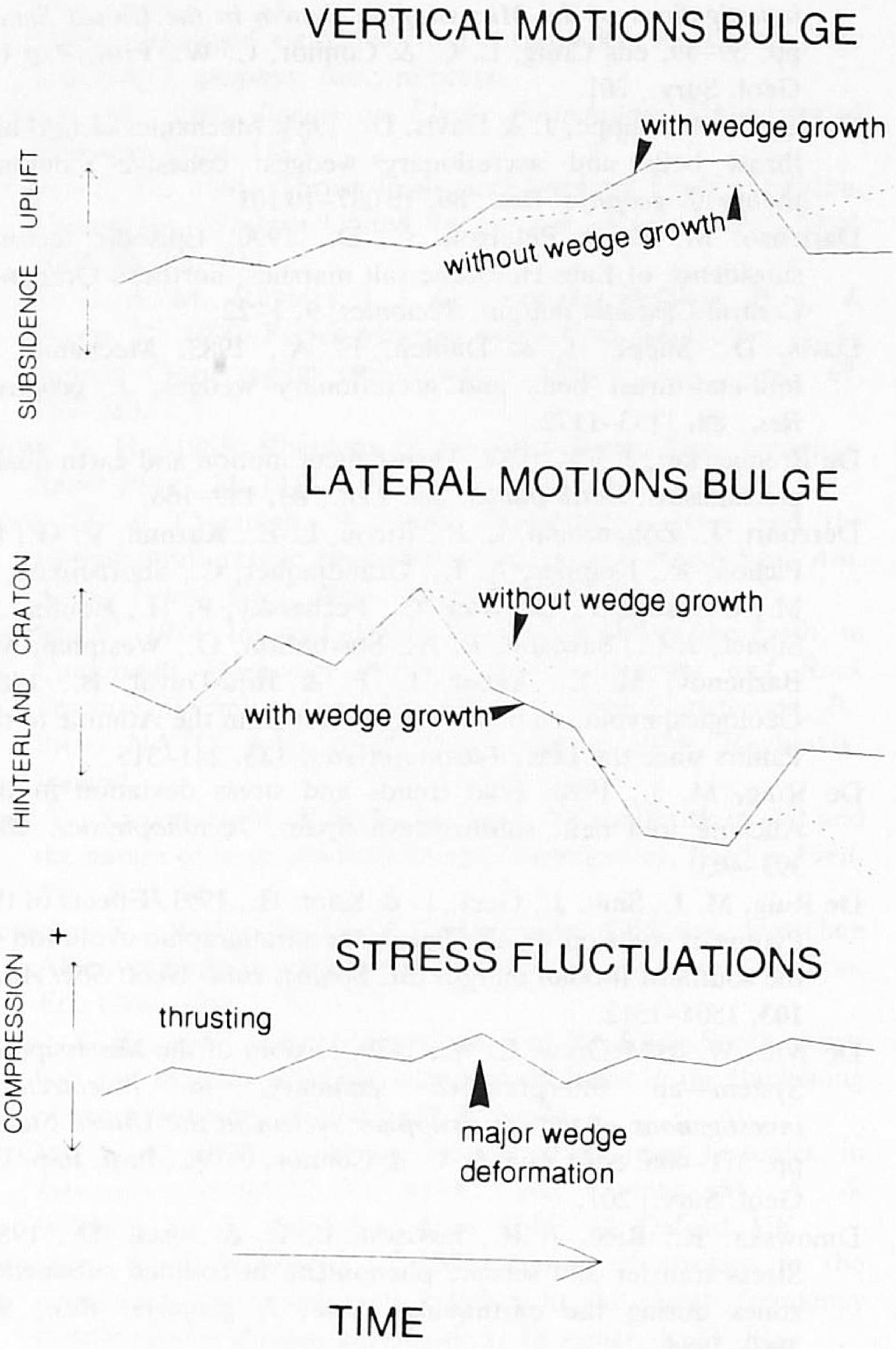

Figure 23. Schematic display of the changes of the response of the lithosphere to growth of the accretionary wedge with time. The dashed lines show postulated bulge motions without incorporation of the effects of wedge growth; the continuous lines indicate the bulge motions caused by a change of the effect of thrusting and stress fluctuations due to wedge growth. The vertical motions due to stress fluctuations become more significant, while the effect of thrusting becomes smaller with time.

flexural state of the foreland basins and the role of the flexural state of the basins in adjacent areas is concerned, vertical motions of the lithosphere are dependent of the dominance of the flexural waves of either the thrust load or the adjacent basin. In cases of a relatively large deflection of the peripheral basin, bulge migrations will be determined by the vertical motions in the peripheral basin, while the opposite occurs with a relatively large deflection of the thrust load. Since both basins are subject to changes with time, the response of the lithosphere also changes with time, complicating the depositional history of the basin.

The time-scale of the processes, and also the kinematics of readjustments of the thrust configuration related to stress, are determined by the rheological properties of the lithosphere. This is because the amount of time that passes without thrusting taking place, and thus with stress levels to increase, depends on the shear strength of the rocks. Apart from this dynamic aspect, the kinematics of the geometry of the thrust wedge are also affected by the rheological properties, because the lateral and vertical extent of the nappes, which build up the wedge, are controlled by the shear strength. This again has its feed back to the dynamics of the wedge, as thrusting changes the spatial distribution of strata in the wedge, leading to a reorganization of the rheological build up of the wedge.

The rheological properties, however, do not only change as a consequence of thrust displacement, changing the rheological build up of the wedge. In general, the underthrusted lithosphere has also inherited a lateral variation of rheological properties from earlier tectonic processes (Ranalli & Murphy 1987; Ziegler 1990). Earlier rift phases for example may have induced a lateral thinning of crustal layers, affecting the scale of thrust formation (e.g. Ord & Hobbs 1989). Furthermore, as zones with lateral variations in rheological properties migrate towards the centre of the collision belt with time, rheologically different units get involved in the orogeny, with time. Since the rheological properties of the lithosphere thus change with lateral and vertical reorganizations of the lithosphere related to thrusting and folding, the process of progressive deformation substantially contributes to the observed complex patterns of vertical motions in foreland basins.

CONCLUSIONS

The conceptual model for vertical motions in foreland basins presented in this paper provides an alternative dynamic mechanism for the deposition of third and higher order on- and off-lap sequences, which has often been explained by short-term eustatic sea-level fluctuations. Similarly, the model explains a large spectrum of longer term vertical motions, part of which has previously been attributed to visco-elastic models. The magnitude and the duration of the vertical motions reflects the scale of deformation and associated stress accumulation. Short-term vertical motions are the result of small-scale thrust events, while long-term motions appear to be the consequence of larger scale deformation of the accretionary wedge.

The expression of stress fluctuations and thrusting in the stratigraphic record is controlled by the presence and the size of a peripheral basin, the value of the effective elastic thickness of the underthrusted lithosphere, and the volume and the shape of the overriding pile of nappes. The changes of the basin with time are strongly affected by the rheological properties of the units involved in the process.

ACKNOWLEDGMENTS

J. Melosh is gratefully acknowledged for providing the initial version of the TECTON code. R. Stephenson, H. Kooi, J. D. van Wees, R. Zoetemeijer and G. Stockmal are thanked for valuable suggestions and fruitful discussions.

REFERENCES

Almendinger, R. W., Figueroa, D., Snyder, D., Beer, J., Mpodozis, C. & Isacks, B. L., 1990. Foreland shortening in the Andes at 30°S latitude, *Tectonics*, **9**, 789–809.

Anderson, E. J., Goodwin, P. W. & Sobieski, T. H., 1984.

Episodic accumulation and the origin of formation boundaries in the Helderberg Group of New York State, *Geology*, **12,** 120–123.

Angevine, C. L., 1989. Relationship of eustatic oscillations to regressions and transgressions on passive continental margins, in *Origin and Evolution of Sedimentary Basins and their Energy and Mineral Resources,* pp. 29–35, ed. Price, R. A., Am. Geophys. Un., Geophy, Monogr., 48, Washington, DC.

Armstrong, F. C. & Oriel, S. S., 1986. Tectonic development of the Idaho–Wyoming thrust belt, *Am. Assoc. Petrol. Geol. Mem.*, **41,** 243–259.

Beaumont, C. B., 1981. Foreland basins, *Geophys. J. R. astr. Soc.*, **65,** 291–329.

Beaumount, C. B., Fulsack, P., Willett, S., Hamilton, J., Johnson, D., Ellis, S. & Paton, M., 1990. Coupling of climate, surface processes and tectonics in orogens and their associated sedimentary basins, in *Lithoprobe East: report of transect meeting, Oct, 1990,* Memorial University, St. John's Newfoundland.

Berger, J. P., 1985. La transgression de la molasse superieure (OMM) a Suisse Occidentale, *Munch. Geowissen. Abh.*: *Riehe A, Geol. Pal.*, **5**.

Berger, A. L., Imbrie, J., Hays, J., Kukla, G. & Salzman, B. (eds), 1984, *Milankovitch and Climate,* Reidel, Boston.

Bergerat, F., Cazes, M., Damotte, B., Guellec, S., Mugnier, J. L., Roure, F. & Truffert, C., 1989. Les structures distensive en Bresse d'apres les donnees du profile sismique Jura-Bresse (programme ECORS), *C. R. Acad. Sci.*, **309,** 325–332.

Birch, F., 1966. Compressibility; elastic constants, in *Handbook of Physical Constants,* pp. 97–174, ed. Clark, S. P., Geol. Soc. Am. Mem., 97, New Haven, Connecticut.

Bodine, J. H., 1981. The thermo-mechanical properties of the oceanic lithosphere, *PhD thesis,* Columbia University, Palisades, New York.

Boyer, S. E. & Elliot, D., 1982. Thrust systems, *Am. Assoc. Petrol. Geol. Bull.*, **60,** 1196–1230.

Byerlee, J., 1978. Friction of rocks, *Pageoph.*, **116,** 615–626.

Cant, D. J. & Stockmal, G. S., 1989. The Alberta foreland basin, relationship between stratigraphy and Cordillera terrane accretion events, *Can. J. Earth Sci.*, **26,** 1964–1975.

Carter, N. L. & Tsenn, M. C., 1987. Flow properties of continental lithosphere, *Tectonophysics*, **136,** 27–63.

Cloetingh, S., 1988. Intraplate stresses: a new element in basin analyses, in *New Perspectives in Basin Analyses,* pp. 205–230, eds Kleinspehn, K. L. & Paola, C., Springer, New York.

Cloetingh, S., 1991. Tectonics and sea-level changes: a controversy? in *Controversies in Modern Geology,* pp. 250–277 eds Mueller, D., McKenzie, J. & Weissert, H., Academic Press, London.

Cloetingh, S. & Wortel, M. J. R., 1986. Stress in the Indo-Australian plate, *Tectonophysics,* **132,** 49–67.

Cloetingh, S., McQueen, H. & Lambeck, K., 1985. On a tectonic mechanism for regional sealevel variations, *Earth planet. Sci. Lett.*, **75,** 157–166.

Cloetingh, S., Kooi, H. & Groenewoud, W., 1989. Intraplate stresses and sedimentary basin evolution, in *Origin and Evolution of Sedimentary Basins and their Energy and Mineral Resources,* pp. 1–16, ed. Price, R. A., Am. Geophys. Un., Geophys. Monogr., 48, Washington, DC.

Cochran, J. R., 1990. Himalayan uplift, sealevel and the record of the Bengal fan sedimentation at the ODP leg 116 Sites, *Proc. ODP Sci. Res.*, **116,** 261–277.

Courtney, R. C. & Beaumont, C., 1983. Thermally-activated creep and flexure of the oceanic lithosphere, *Nature,* **305,** 201–204.

Cowie, P. A. & Scholz, C. H., 1991. Relationship between scaling laws for earthquakes and growth of faults by accumulation of earthquake slips, *Terra Abstracts, Strasbourg 1991,* 153.

Craig, L. C. & Varnes, K. L., 1979. History of the Mississippian system—An interpretative summary, in *Paleotectonic investigations of the Mississippian System in the United States,* pp. 39–49, eds Craig, L. C. & Connor, C. W., Prof. Pap US Geol. Surv., 201.

Dahlen, F. A., Suppe, J. & Davis, D., 1984. Mechanics of fold-and thrust belts and accretionary wedges: cohesive Coulomb theory, *J. geophys. Res.*, **89,** 10 087–10 101.

Darienzo, M. E. & Peterson, C. D., 1990. Episodic tectonic subsidence of Late Holocene salt marshes, northern Oregon—Central Cascadia margin, *Tectonics*, **9,** 1–22.

Davis, D., Suppe, J. & Dahlen, F. A., 1983. Mechanics of fold-and-thrust belts and accretionary wedges, *J. geophys. Res.*, **88,** 1153–1172.

De Bremaecker, J. Cl., 1987. Thrust sheet motion and earth quake mechanisms, *Earth planet. Sci. Lett.*, **83,** 159–166.

Dercourt, J., Zonenshain, L. P., Ricou, L.-E., Kazmin, V. G., Le Pichon, X., Knipper, A. L., Grandjaquet, C., Sbortshikov, I. M., Geyssant, J., Lepvrier, C., Pechersky, P. H., Boulin, J., Sibuet, J.-C., Savostin, L. A., Sosrokhtin, O., Westphal, M., Bazhenov, M. L., Lauer, L. P. & Biju-Duval, B., 1986. Geological evolution of the Tethys belt from the Atlantic to the Pamirs since the Lias, *Tectonophysics,* **123,** 241–315.

De Ruig, M. J., 1990. Fold trends and stress deviation in the Alicante fold belt, southeastern Spain, *Tectonophysics,* **184,** 393–403.

De Ruig, M. J., Smit, J., Geel, T. & Kooi, H., 1991. Effects of the Pyrenean collision on the Paleocene stratigraphic evolution of the southern Iberian margin (SE Spain), *Bull. Geol. Soc. Am.*, **103,** 1504–1512.

De Witt, W. & McGrew, L. W., 1979. History of the Mississippian System—an interpretative summary, in *Paleotectonic investigations of the Mississippian System in the United States,* pp. 371–406, eds Craig, L. C. & Connor, C. W., Prof. Pap. US Geol. Surv., 201.

Dmowska, R., Rice, J. R., Lovison, L. C. & Josell, D., 1988. Stress transfer and seismic phenomena in coupled subduction zones during the earthquake cycle, *J. geophys. Res.*, **93,** 7869–7884.

Dorobek, S. L., Reid, S. K., Elrick, M., Bond, G. C. & Kominz, M. A., 1992. Foreland response to episodic convergence: subsidence history of the Antler foredeep and adjacent cratonic platform areas, Montana and Idaho, in *Sedimentary Modeling: Computer Simulation and Methods for Improved Parameter Definition,* eds Franseen, E. & Watney, L., Kansas Geol. Soc. Spec. vol, in press.

ECORS Pyrenees Team, 1988. The ECORS deep reflection seismic survey across the Pyrenees, *Nature,* **331,** 508–511.

Embry, A. F., 1989. A tectonic origin for third-order depositional sequences in extensional basins—implications for basin modelling, in *Quantitative Dynamic Stratigraphy,* pp. 491–502, ed. Cross, T. A., Prentice Hall, New Jersey.

Evans, K., 1989. Appalachian stress study 3. Regional scale stress variations and their relation to structure and contemporary tectonics, *J. geophys. Res.*, **94,** 17 619–17 645.

Flemmings, P. B. & Jordan, T. E., 1989. A synthetic stratigraphic model of foreland basin development, *J. geophys. Res.*, **94,** 3851–3866.

Galloway, W. E., 1989. Clastic facies models, depositional systems, sequences and correlation: a sedimentologists's view of the dimensional and temporal resolution of lithostratigraphy, in *Quantitative Dynamic Stratigraphy,* pp. 113–126, ed. Cross, T. A., Prentice Hall, New Jersey.

Glacon, G. & Rouvier, M., 1972. Ages des mouvements tectoniques majeurs en Tunesie septentrionale, *C. R. Acad. Sci.*, **274,** 1257–1260.

Goetze, C. & Evans, B., 1979. Stress and temperature in the bending lithosphere as constrained by experimental rock mechanics, *Geophys. J. R. astr. Soc.*, **59,** 463–478.

Govers, R., Wortel, M. J. R., Gloetingh, S. & Stein, C. A., 1992.

Stress magnitude estimates from earthquakes in oceanic plate interiors, *J. geophys. Res.*, in press.

Hetenyi, M., 1946. *Beams on Elastic Foundation*, University of Michigan Press, USA.

Jordan, T. E., 1981. Thrust loads and foreland basin evolution, Cretaceous, Western United States, *Am. Assoc. Petrol. Geol. Bull*, **70,** 396–414.

Kenter, J. A. M., Reymer, J. J. G., Van der Straaten, H. C. & Peper, T., 1990. Facies patterns and subsidence history of the Jumilla-Cieza region (southeastern Spain), *Sed. Geol.*, **67,** 263–280.

Kirby, S. H., 1983. Rheology of the lithosphere, *Rev. Geophys. Space Phys.*, **21,** 1458–1487.

Kooi, H. & Cloetingh, S., 1989. Intraplate stresses and the tectono-stratigraphic evolution of the central North Sea, *Am. Assoc. Petrol. Geol. Mem.*, **46,** 541–558.

Kröner, E., 1974. Internal stresses in crystals and in the earth, in *Continuum Mechanics Aspects of Geodynamics and Rock Fracture Mechanics*, pp. 135–150, ed. Thoft-Christensen, P., Proc. NATO Adv. Stud. Inst. August 1974, Reykjavik, Iceland.

Lay, T., Kanamori, H. & Ruff, R., 1982. The asperity model and the nature of large subduction zone earthquakes, *Earthq. Pred. Res.*, **1,** 3–71.

Lemcke, K., 1981. Das heutige geologische Bild des deutschen Alpenvorlandes nach drei Jahrzehnten Ölund Gasexploration, *Ecl. Geol. Helv.*, **74,** 1–18.

Lucas, S. B., 1989. Structural evolution of the Cape Smith thrust belt and the role of out-of-sequence thrusting in the thickening of mountain belts, *Tectonics*, **7,** 655–676.

McClay, K. R., 1989. Analogue models of inversion tectonics, in *Inversion Tectonics*, pp. 41–62, eds Cooper, M. A. & Williams, G. D., Geol. Soc. Spec. Publ., 44, Oxford, UK.

Meissner, R. & Strehlau, J., 1982. Limits of stresses in the continental crust and their relation to the depth–frequency distribution of shallow earthquakes, *Tectonics*, **1,** 73–79.

Melosh, H. J. & Raefsky, A., 1981. A simple and efficient method for introducing faults into finite element computations, *Bull. seism. Soc. Am.*, **71,** 1391–1400.

Mercier, J. L., 1992. Neogene stress changes in the Andean chain, *J. geophys. Res.*, in press.

Mitchell, A. H. G., 1984. Initiation of subduction by post-collision foreland thrusting and backthrusting, *J. Geod.*, **1,** 103–120.

Monger, J. W. H., 1989. Overview of Cordilleran geology, in *Western Canada basin—a case history*, pp. 9–32, ed. Rickets, B. D., Can. Soc. Petrol. Geol. Spec. vol, Calgary, Alta.

Monger, J. W. H. & Price, R. A., 1979. The geodynamic evolution of the Canadian Cordillera—progress and problems, *Can. J. Earth Sci.*, **16,** 770–791.

Monnier, F., 1979. Correlations mineralogiques et diagenese dans le basin molassique Suisse, *These*, Neuchatel.

Morley, C. K., 1986. A classification of thrust fronts, *Am. Assoc. Petrol. Geol. Bull.*, **70,** 12–25.

Morley, C. K., 1988. Out-of-sequence thrusts, *Tectonics*, **7,** 539–561.

Mugnier, J. L. & Menard, G., 1986. Le developpement du basin molassique suisse et l'evolution des Alpes externes: une modele cinematique [The development of the Swiss Molasse basin and the evolution of the external Alpes: a kinematic model], *Bull. Centres Rech. Explor.-Prod. Elf-Aquitane*, **10,** 167–180.

Nemec, W., 1988. Coal correlations and intrabasinal subsidence: a new analytical perspective, in *New Perspectives in Basin Analyses*, pp. 161–188, eds Kleinspehn, K. L. & Paola, C., Springer, New York.

Ord, A. & Hobbs, B. E., 1989. The strength of the continental crust, detachment zones and the development of plastic instabilities, *Tectonophysics*, **158,** 269–289.

Peper, T. & Cloetingh, S., 1992. Lithosphere dynamics and tectono-stratigraphic evolution of the Mesozoic Iberian rifted margin (southeastern Spain), *Tectonophysics*, **203,** 345–361.

Pfiffner, O. A., 1986. Evolution of the north Alpine foreland basin in the central Alps, in *Foreland Basins*, pp. 219–228, eds Allen, P. A. & Homewood, P., Spec. Publ. Int. Ass. Sed., 8 Blackwell, Oxford.

Pfiffner, O. A., Frei, W., Valasek, P., Stauble, M., Levato, L., Du Bois, L., Schmid, S. M. & Smithson, S. B., 1990. Crustal shortening in the Alpine orogen: results from deep seismic reflection profiling in the eastern Swiss Alps, line NFP 20-east, *Tectonics*, **9,** 1327–1355.

Posamentier, H. W., Jervey, M. T. & Vail, P. L., 1988. Eustatic controls on clastic deposition I—conceptual framework, in *Sea-Level Changes—An Integrated Approach*, pp. 47–69, eds Wylgus, C. K., Hastings, B. S., Kendall, C. G. St. C., Posamentier, H. W., Ross, C. A. & Van Wagoner, J. C., Soc. Ec. Pal. Min. Spec. Publ., 42, Tulsa, Oklahoma.

Price, R. A., 1986. The southeastern Canadian Cordillera: Thrust faulting, tectonic wedging and delamination of the lithosphere, *J. Struct. Geol.*, **8,** 239–254.

Price, R. A., Monger, J. W. H. & Muller, J. E., 1981. Cordilleran cross-section, Calgary to Victoria, in *Field Guides to Geological and Mineralogical Deposits: Calgary*, eds Thompson, R. I. & Cook, D. G., Geol. Soc. Can.

Quinlan, G. M. & Beaumont, C., 1984. Appalachian thrusting, lithosphere flexure and the Paleozoic stratigraphy of the eastern interior of North America, *Can. J. Earth Sci.*, **21,** 973–996.

Ranalli, G., 1989. *Rheology of the Earth*, Allen & Unwin, Boston.

Ranalli, G. & Murphy, D. C., 1987. Rheological stratification of the lithosphere, *Tectonophysics*, **132,** 281–295.

Schedl, D. V. & Dorr, J. A., 1983. Timing of deformation in overthrust belt and foreland of Idaho Wyoming and Utah, *Am. Assoc. Petrol. Geol. Bull.*, **67,** 1304–1322.

Schedl, A. & Wiltschko, D. V., 1984. Sedimentological effects of a moving terrain, *J. Geol.*, **92,** 273–287.

Schedl, A. & Wiltschko, D. V., 1987. Possible effects of pre-existing basement topography on thrust fault ramping, *J. Struct. Geol*, **9,** 1029–1037.

Sclater, J. G. & Christie, P. A. F., 1980. Continental Stretching: an explanation of the post-mid-Cretaceous subsidence of the central North Sea basin, *J. geophys. Res.*, **85,** 3711–3739.

Searle, M. P., 1985. Sequence of thrusting and origin of culminations in the northern and central Oman Mountains, *J. Struct. Geol.*, **7,** 129–143.

Sibson, R. H., 1986. Brecciation processes in fault zones: Interference from earthquake rupturing, in *Internal Structure of Fault Zones*, pp. 159–176, ed. Wang, Ch.-Y., Pageoph., 124, Basel.

Silver, E. A. & Reed, D. L., 1988. Backthrusting in accretionary wedges, *J. geophys. Res.*, **93,** 3116–3126.

Silver, E. A., Reed, D. L., McCaffrey, R. & Joyodiwiryo, Y., 1983. Back arc thrusting in the eastern Sunda arc, Indonesia: A consequence of arc-continent collision, *J. geophys. Res.*, **88,** 7429–7448.

Sinclair, H. D., Coakley, B. J., Allen, P. A. & Watts, A. B., 1991. Simulation of foreland basin stratigraphy using a diffusion model of mountain belt uplift and erosion: an example from the Central Alps, Switzerland, *Tectonics*, **10,** 599–620.

Stein, C. A., Cloetingh, S. & Wortel, R., 1990. Kinematics and mechanics of the Indian Ocean diffuse plate boundary zone, *Proc. ODP Sci. Res.*, **116,** 261–277

Stel, H., 1986. The effect of cyclic operation of brittle and ductile deformation on the metamorphic assemblage in cataclasites and mylonites, in *Internal Structure of Fault zones*, pp. 159–176, ed. Wang, Ch-Y., Pageoph, 124, Basel.

Stephenson, R., 1989. Beyond first order thermal subsidence models for sedimentary basins? in *Quantitative Dynamic*

Stratigraphy, pp. 113–126, ed. Cross, T. A., Prentice Hall, New Jersey.
Stephenson, R. & Cloetingh, S., 1991. Some examples and mechanical aspects of continental lithosphere folding, *Tectonophysics,* **188,** 27–37.
Stern, T. A. & Davey, F. J., 1990. Deep seismic expression of a foreland basin: Taranaki basin, New Zealand, *Geology,* **18,** 979–982.
Stockmal, G. S. & Beaumont, C., 1987. Geodynamic models of convergent margin tectonics: the southern Canadian Cordillera and the Swiss Alps, in *Sedimentary Basin and Basin-forming Mechanisms,* pp. 393–411, eds Beaumont, C. & Tankard, A. J., Can. Soc. Petrol. Geol. Mem., 12, Calgary, Alberta.
Stockmal, G. S., Beaumont, C. & Boutelier, R., 1986. Geodynamic models of convergent margin tectonics: the transition from rifted margin to overthrust belt and the consequences for foreland basin development, *Am. Assoc. Petrol. Geol. Bull.,* **70,** 181–190.
Suppe, J., 1985. *Principles of Structural Geology,* Prentice Hall, New Jersey.
Tankard, A. J., 1986a. Depositional response to foreland deformation in the Carboniferous of eastern Kentucky, *Am. Assoc. Petrol. Geol. Bull.,* **70,** 853–868.
Tankard, A. J., 1986b. On the depositional response to thrusting and lithospheric flexure: examples from the Appalachian and Rocky Mountain basins, in *Foreland Basins,* pp. 369–392, eds Allen, P. A. & Homewood, P., Spec. Publ. Int. Ass. Sed., 8 Blackwell, Oxford.
Taylor, F. W., Lawrence Edwards, R., Wasserburg, G. J. & Frohlich, C., 1990. Seismic recurrence intervals and timing of a seismic subduction inferred from emerged corals and reefs of the Central Vanuatu (New Hebrides) frontal arc, *J. geophys. Res.,* **95,** 393–408.
Thorne, J. A. & Watts, A. B., 1989. Quantitative analysis of North Sea subsidence, *Am. Assoc. Petrol. Geol. Bull.,* **73,** 88–116.
Vail, P., Mitchum Jr, R. M. & Thompson III, S., 1977. Global cycles of relative changes of sea level, *Am. Assoc. Petrol. Geol. Mem.,* **26,** 83–97.
Van Wagoner, J. C., Mitchum, R. M., Campion, K. M. & Rahmanian, V. D., 1990. Siliciclastic sequence stratigraphy in well logs, cores, and outcrops, *Am. Assoc. Petrol. Geol. Expl. Ser.,* **7.**
Van Wees, J. D. & Cloetingh, S., 1991. Finite element models for basin extension and inversion, in *Abstract of Special meeting of the Geological Society of France: Analysis and modelling of faulting,* p. 72.
Walcott, R. I., 1976. Lithospheric flexure, analysis and gravity anomalies and the propagation of seamount chains, in *The Geophysics of the Pacific Ocean Basin and its Margin,* pp. 431–438, eds Sutton *et al.,* Am. Geophys. Un. Geophys. Monogr., 19, Washington, DC.
Watts, A. B., Karner, G. D. & Steckler, M. S., 1982. Lithospheric flexure and the evolution of sedimentary basins, *Phil. Trans. R. Soc. Lond. A,* **305,** 249–281.
Ziegler, P. A., 1990. *Geological Atlas of Western and Central Europe,* (second revised edition), Shell Int. Petrol. Maatsch, The Hague/ Geol. Soc. London.
Zoback, M. L., *et al.* (World Stress map team), 1989. Global patterns of tectonic stress, *Nature,* **341,** 291–298.

APPENDIX

As shown by Walcott (1976) and Hetenyi (1946) the flexual response of a broken plate to loading is compatible to that of a continuous plate. Equations (A1) and (A2) govern the deflection of (end) loading of a broken plate and a continuous plate, respectively.

$$w_b = \frac{q\lambda^2}{2k} e^{-\alpha x} \frac{2\alpha\beta \cos(\beta x) + (\alpha^2 - \beta^2)\sin(\beta x)}{\beta(3\alpha^2 - \beta^2)}, \tag{A1}$$

$$w_c = \frac{q\lambda^2}{2k} e^{-\alpha x} \frac{\beta \cos(\beta x) + \alpha \sin(\beta x)}{\alpha\beta}, \tag{A2}$$

$$\lambda = \sqrt{\frac{k}{4D}}, \quad \alpha = \sqrt{\lambda^2 + \frac{N}{4D}}, \quad \beta = \sqrt{\lambda^2 - \frac{N}{4D}}, \tag{A3}$$

where: w_b is the deflection for a broken plate; w_c is the deflection for a continuous plate; q is the vertical force; k is Hooke's constant; D is the flexural rigidity (see equation 2); x is the distance from load; and N is the horizontal stress. Substitution of $N = 0$ gives a two times larger value for the deflection under a line load of a broken plate than for a continuous plate. The roots for equations (A1) and (A2) are found with

$$\frac{-2\alpha\beta}{\alpha^2 - \beta^2} = tg(\beta x_b), \quad x_b = \frac{1}{\beta} \operatorname{arc} tg\left(\frac{-2\alpha\beta}{\alpha^2 - \beta^2}\right), \tag{A4}$$

$$-\frac{\beta}{\alpha} = tg(\beta x_c), \quad x_c = \frac{1}{\beta} \operatorname{arc} tg\left(-\frac{\beta}{\alpha}\right), \tag{A5}$$

where x_b is the root of broken plate equation, and x_c is the root of continuous plate equation.

Equations (A1) and (A2) show that the flexural wavelength of the lithosphere depends on the magnitude of stress, as α and β depend on N. Differences between the changes of the flexural wavelength for a broken plate model and changes for a continuous plate model can be described with the ratio of x_b and x_c. If the ratio remains constant with stress increase, there is no significant difference in the change of the flexural wavelength upon stress, in the different models. For the case of end loading in a broken plate model

$$\frac{x_b}{x_c} = \frac{\operatorname{arc} tg\left(\frac{-2\alpha\beta}{\alpha^2 - \beta^2}\right)}{\operatorname{arc} tg\left(-\frac{\beta}{\alpha}\right)} \tag{A6}$$

a ratio which does not change upon a stress increase of 10 to 10^4 MPa.

Loading at increasing distances from the free end in a broken plate model approaches loading in a continuous plate configuration. In this configuration the ratio of x_b and x_c does not change at all. Extrapolation of the results, therefore, gives that the changes of the ratio converge to zero with increasing distances of loading from the free end in the broken plate model. Consequently, changes upon stress and loading, predicted by continuous plate models, converge to changes in broken plate models, implying that the presented modelling results can also be invoked for broken plate configurations.